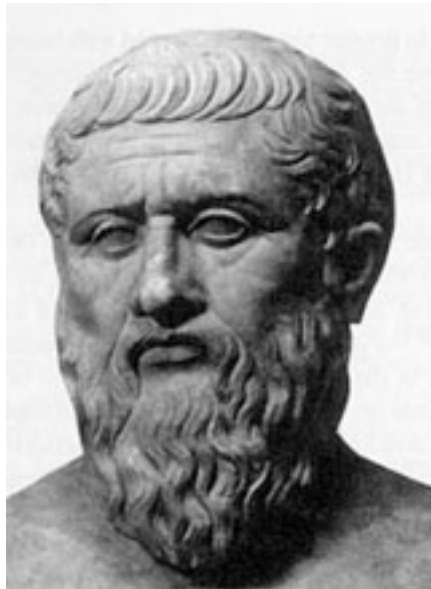


PLATO

PLAnetary Transits and Oscillations of stars

A study of exoplanetary systems

C. Catala and the PLATO consortium



πλατωνι

A proposal for a class-M mission in response to the ESA Cosmic Vision 2015 – 2025
announcement of opportunity

The PLATO consortium:

Observatoire de Paris, France: **G. Alecian, M. Auvergne, A. Baglin, C. Barban, C. Catala, M. Floquet, M.J. Goupil, A.M. Hubert, D. Katz, Y. Lebreton, C. Martayan, E. Michel, B. Mosser, C. Neiner, D. Rouan, R. Samadi**
Institut d'Astrophysique Spatiale, Orsay, France: **T. Apourchaux, F. Baudin, P. Boumier, A. Léger, M. Ollivier**
Observatoire Astronomique Marseille-Provence, France: **J.-C. Bouret, P. Barge, M. Deleuil, C. Moutou**
Observatoire Midi-Pyrénées, Toulouse, France: **T. Böhm, S. Charpinet, N. Dolez, J.F. Donati, P. Fouqué, F. Lignières, P. Petit, M. Rieutord, G. Vauclair, S. Vauclair**
Institut d'Astrophysique de Paris, France: **R. Ferlet, A. Lecavelier, A. Vidal-Madjar**
Service d'Astrophysique/DAPNIA, CEA, Saclay, France: **R. Garcia, S. Turck-Chièze**
Observatoire de la Côte d'Azur, Nice, France: **T. Guillot, P. Mathias**
Katholieke Universiteit Leuven, Belgium: **C. Aerts, M. Briquet, F. Carrier, J. De Ridder, R. Drummond, R. Oestensen**
Université de Liège, Belgium: **A. Noels, A. Thoul**
University of Exeter, UK: **S. Aigrain**
University of St-Andrews, Scotland, UK: **A. Collier Cameron, K. Horne**
Queen Mary, University of London, UK: **I. Roxburgh**
University of Leicester, UK: **M. Barstow**
University of Central Lancashire, UK: **D. Kurtz**
University of Sheffield, UK: **V. Dhillon, M. Thompson**
University of Warwick, UK: **P. Wheatley**
Aarhus Universitet, Denmark: **T. Arentoft, J. Christensen-Dalsgaard, H. Kjeldsen**
Osservatorio Astronomico di Brera, Merate, Italy: **E. Antonello, E. Poretti**
Osservatorio Astrofisico di Catania, Italy: **G. Cutispoto, A. Lanza, G. Leto, S. Messina, I. Pagano, S. Scuderi**
Catania University, Italy: **A. Lanzafame**
Padova University, Italy: **V. Granata, S. Ortolani, G. Piotto**
Osservatorio Astronomico di Padova, Italy: **S. Benatti, R. Claudi, S. Desidera**
Osservatorio Astronomico di Capodimonte, Italy: **D. De Martino, M. Marconi, I. Musella, V. Ripepi, R. Silvotti, A. Vittone**
Instituto de Astrofísica de Canarias, Spain: **J.A. Belmonte, H. Deeg, E. Martin, C. Regulo Rodriguez, R. Simoniello**
Instituto de Astrofísica de Andalucía, Granada, Spain: **R. Garrido, A. Moya, J.C. Suarez, E. Rodriguez, S. Martin-Ruiz, P. Amado, C. Rodriguez-Lopez, A. Garcia**
Centro de Astrobiología (CSIC-INTA), Madrid, Spain: **M. Mass Hesse**
University of Barcelona, Spain: **I. Ribas**
University of Valencia, Spain: **J. Fabregat, J. Gutierrez-Soto, J. Suso, P. Diago**
Universidade do Porto, Portugal: **M. Cunha, J. Gameiro, M. Monteiro, N. Santos, C. Straka**
DLR, Berlin, Germany: **A. Erikson, H. Rauer**
Thüringer Landessternwarte Tautenburg, Germany: **G. Wuchterl**
Astrophysikalisches Institut Potsdam, Germany: **K. Strassmeier**
Max Planck Institute for Astrophysics, Garching, Germany: **J. Ballot**
Universität Wien, Austria: **G. Handler, W. Weiss**
Observatoire de Genève, Switzerland: **M. Mayor, G. Meynet, D. Queloz**
RSSD, ESA: **C. Isola** (Research Fellow)
Caltech, Michelson Science Center, USA: **C. Beichman, D. Ciardi, G. Van Belle**
Jet Propulsion Laboratory, USA: **J. Hong, W. Traub**
Caltech, Spitzer Science Center, USA: **J. Stauffer**
Yale University, USA: **S. Basu**
National Solar Observatory, USA: **J. Leibacher**
ARIES, Nainital, India: **R. Sagar**
University of Mumbai, India: **K. Chitre**
Indian Institute of Astronomy and Astrophysics, Bangalore, India: **S. Hasan**
University of Sao Paulo, Brazil: **E. Janot Pacheco**
Universidade Federal do Rio Grande do Norte, Brazil: **J. Renan de Medeiros**
Universidade Federal do Rio de Janeiro, Brazil: **G. Porto de Mello, H. Rocha Pinto**

PLATO Mission Concepts

scientific objectives	discover and characterize a large number of close-by exoplanetary systems
primary data product	simultaneous, accurate, long duration light curves of large number of stars
payload concept	ultra-precise, very wide field optical photometer

'staring' concept

observing plan	4 years of continuous monitoring of a single field + 1 year of 'step and stare' monitoring of 12 fields for 1 month each
duty cycle	> 95%

'spinning' concept

observing plan	5-year operation. 6 months per year in search mode + 6 months per year in fine mode
duty cycle	5% in search mode, > 95% in fine mode

Payload

'staring' concept

telescopes	100 identical 100 mm pupil telescopes with 26° field
focal planes	100 identical 24-CCD focal planes, with 800 × 1800 × 13μm CCDs
performance	2.5 10 ⁻⁵ (1 ppm in 30 d) photometric noise level in 1 hr at m _V = 11 – 12
number of stars	100,000 stars with 2.5 10 ⁻⁵ noise level in 1 hr, m _V ≤ 11 – 12 360,000 stars with 8 10 ⁻⁵ noise level in 1 hr, m _V ≤ 14
science performance	detect sub-earth-size planets around solar-type stars down to m _V = 11 – 12 detect earth-size planets around early-F, late-A stars down to m _V = 11 – 12 detect earth-size planets around solar-type stars down to m _V = 14 measure solar-like oscillations down to m _V = 11 – 12 measure oscillations of classical pulsators down to m _V = 14

'spinning' concept

telescopes	3 identical 0.72 m ² telescopes with 5.9 × 3.9° field
focal planes	3 identical 32 CCD focal planes, with <i>Gaia</i> -type 4500 × 2000 CCDs
performance	8 10 ⁻⁵ photometric noise level in 1 hr at m _V = 11 in search mode 2.5 10 ⁻⁵ (1ppm in 30d) noise level in 1 hr at m _V = 11 in fine mode
number of stars	144,000 stars with 8 10 ⁻⁵ noise level in 1 hr, m _V ≤ 11 in search mode 240,000 stars with 1.3 10 ⁻⁴ noise level in 1 hr, m _V ≤ 14 in search mode 85,000 stars with 2.5 10 ⁻⁵ noise level in 1 hr, m _V ≤ 11 in fine mode
science performance	detect earth-size planets around solar-type stars down to m _V = 11 – 12 detect super-earth-size planets around solar-type stars down to m _V = 14 measure solar-like oscillations down to m _V = 11 – 12 in fine mode measure oscillations of classical pulsators down to m _V = 14 in all modes

Spacecraft

'staring' concept

service module	<i>Herschel</i> recurrent platform
pointing stability	0.2"
telemetry	200 kbits/s sustained payload telemetry rate

'spinning' concept

service module	<i>Gaia</i> recurrent platform
pointing stability	0.2" in fine mode, spinning period 20 min in search mode
telemetry	130 kbits/s sustained payload telemetry rate

Orbit, Launch, and Lifetime

orbit	large Lissajous around L2
launch	single Soyuz-Fregat launch from Kourou
lifetime	≥ 5 years

Executive summary

The *PLAnetary Transits and Oscillations of stars* Mission (PLATO) will detect and characterize exoplanets by means of their transit signature in front of a very large sample of bright stars, and measure the seismic oscillations of the parent stars orbited by these planets in order to understand the properties of the exoplanetary systems. PLATO is the next-generation planet finder, building on the accomplishments of CoRoT and *Kepler*: *i*) it will observe significantly more stars, *ii*) which will be three magnitudes brighter (hence the precision of the measurements will be correspondingly greater as will be those of post-detection investigations, *e.g.* spectroscopy, asteroseismology, and eventually imaging), *iii*) it will be capable of observing significantly smaller exoplanets, *iv*) with significantly longer orbital periods. The space-based observations will be complemented by ground- and space-based follow-up observations; for instance spectroscopic measurements of radial velocities of the detected exoplanetary systems will be obtained to derive the planet masses; differential visible and infrared spectroscopy during and outside secondary transit will also be performed, in particular with JWST, in order to derive information on the exoplanet atmospheres. An ancillary scientific outcome of PLATO will be an unprecedented database for the study of variable stars and stellar internal structure and evolution using asteroseismology down to ppm level, on all time scales from seconds to years, on all types of stars.

These goals will be achieved by a long-term, high-precision, high-time-resolution, high-duty-cycle monitoring in visible photometry of a sample of more than 100,000 relatively bright ($m_V \leq 12$) stars and another 400,000 down to $m_V = 14$. In order to achieve its objectives, the PLATO mission must meet several stringent science requirements:

- *Field-of-view*: the search for planetary transits around bright stars requires a very wide field in order to achieve a significant number of detections given the relatively small density of bright stars in the sky – more than about 300 degree², in order to include more than 100,000 such stars. This strategy is in contrast to previous approaches, such as CoRoT, *Kepler* or *Edgington*, which are or were designed to survey a large volume of the Galaxy by observing fainter and more distant stars in a smaller field.

- *Duration*: in order to detect and characterize planets with orbital periods up to one year, the duration of the monitoring to be performed must be at least three, and

preferably five, years.

- *Photometric noise level*: photometric noise levels as low as 8×10^{-5} (goal 2.5×10^{-5}) in one hour for stars of $m_V=11-12$ are necessary for detecting planets down to the size of the Earth, while a resulting photometric noise level in Fourier space of one ppm in 30 days for stars with $m_V = 11-12$ is a prerequisite for asteroseismology of solar-like stars in the same sample. A total collecting area of the order of 0.7–0.8 m² is needed to meet these requirements.

With the help of Thales-Alenia-Space and Astrium Satellites, we propose two different mission concepts for PLATO: *i*) a “staring” concept with one hundred small, very wide-field telescopes, assembled on a single platform and all looking at the same 26° diameter field, and *ii*) a “spinning” concept with three moderate-size telescopes covering more than 1400 degree². In both concepts the mission would be launched and injected into an L2 orbit by a Soyuz-Fregat rocket.

The “staring concept” utilizes 100 telescopes each with its own CCD focal plane, comprised of 24 CCDs with 800×1800 pixels, operated in full-frame mode, which monitors the same field for the entire mission, *i.e.* up to five years. The satellite is three-axis stabilized and uses a *Planck-Herschel* recurrent platform.

The “spinning” concept uses a *Gaia* platform, and three identical 0.72 m² telescopes, pointing 120° from one another, sweep out a great circle on the sky perpendicular to the spin axis. The payload would also be used half of the time in a fine-pointing mode, during which the spacecraft is three-axis stabilized. The focal plane of each telescope is made up of 32 *Gaia*-type CCDs operated in TDI mode in the spinning phases and in frame transfer mode in the pointed phases.

Both concepts are fully compliant with the science requirements, and give us a strong confidence in the feasibility of this mission. They should be further evaluated at the beginning of the assessment phase, and a choice of concept will be made early in this phase.

PLATO is conceived as a European mission, with a significant contribution from NASA and ISRO. The proposed concept assumes that the spacecraft, launch and operations, as well as a major part of the payload, will be provided by ESA, while the focal planes and the scientific data handling will be provided by a consortium involving the US, India and the European scientific community through national funding by some of ESA member states.

Contents

1	Introduction	4
2	Scientific objectives: evolution of stars and their planetary systems	5
2.1	Studying stars and their planets	5
2.2	Evolution of planetary systems	6
2.3	Stellar evolution	6
2.4	Detection and characterization of planetary transits	7
2.5	Asteroseismology	9
2.6	Follow-up observations	11
2.7	Additional science	12
2.8	Required observations	12
2.8.1	Basic observation strategy	12
2.8.2	The stellar sample	13
2.8.3	Surveyed field	13
2.8.4	Photometric noise level	13
2.8.5	Collecting area and overall throughput	14
2.8.6	Non photonic sources of noise	15
2.8.7	Duration of observations	15
2.8.8	Duty cycle	15
2.8.9	Coloured information	16
2.8.10	Time sampling	16
2.8.11	Dynamical range	17
2.8.12	Summary of observational requirements	17
2.9	The need to go to space	17
3	Mission profile	18
3.1	Orbit	18
3.2	Launcher	19
3.3	Ground station visibility	19
3.4	Mission lifetime	19
3.5	Science operations	19
4	Instrumental concepts	19
4.1	The “staring” concept	19
4.1.1	Observation strategy	19
4.1.2	Proposed payload	20
4.1.3	Expected performance	24
4.1.4	Basic spacecraft characteristics	25
4.1.5	Technological readiness	26
4.1.6	Programmatics and costs	26
4.2	The “spinning” concept	28
4.2.1	Measurement principle	28
4.2.2	Observation strategy	29
4.2.3	Payload definition	29
4.2.4	Expected performance	30
4.2.5	Basic spacecraft characteristics	31
4.2.6	Technological readiness	32
4.2.7	Programmatics and costs	32
4.3	Advantages of the various concepts	32
4.4	Optional concepts	33
5	Comparison with existing & planned missions	33
6	International partnership	34
7	Communication & outreach	35

1 Introduction

The question of the existence of life beyond Earth has been of concern to humanity for several thousand years. A tremendous effort is now being spent, in particular at ESA with *e.g.* the *Aurora* programme, in the search for present and past life in other bodies of the solar system. However, whatever the outcome of this solar system exploration, the search for and study of planetary systems around other stars, and in particular the search for life signatures in exoplanetary systems, is a prerequisite towards generalising our understanding about the distribution of life in the Universe and how it may have arisen on Earth.

Planet formation and evolution theory is at the centre of this problem. In order to understand the origin of life and to determine where life is most likely to exist in the Universe, a full and reliable understanding of planet formation and evolution is an absolute necessity. We need to measure accurately the distribution of planet sizes, masses and orbits, at least down to Earth-sized planets, and to determine which of these exoplanets are likely to be habitable. As importantly, we need to determine the characteristics of their host stars, such as radius, mass, age, and element abundances. The radii and masses of the host stars must be measured accurately in order to provide a precise measurement of sizes and masses of the detected planets, while the ages of the central stars will provide us with an estimate of the ages of their planetary systems. Only then will we be able to relate all characteristics of the planets to the evolutionary history and age of their host stars, and determine under which initial conditions and at what stage of their evolution planets can provide the necessary environment for life.

Terrestrial planets in the habitable zone (*i.e.* the region in the stellar environment where physical conditions are such that water can be present in liquid state) are of particular interest, since they are in principle privileged sites for the apparition of life. However, the complete picture of exoplanet population that we need to obtain in the first place requires a full study of the whole planet size, mass and orbit spectrum.

Today, one decade after the discovery of the first giant exoplanet, the catalog of known exoplanets contains more than 200 members, most of them giant planets on close-in orbits discovered by the radial velocity method. We know only very few lower mass planets, and in spite of the tremendous efforts spent and recent successes, a full statistical analysis of exoplanet down to Earth mass is out of reach of ground-based observational techniques, whose limitations do not leave much

hope to answer the questions raised above.

On the other hand, we are now entering a new era with the recent launch of CoRoT in December 2006 [3], and with the prospect of the *Kepler* launch in 2009 [6]. These missions, CoRoT as a pioneer, then *Kepler* as a follow-up, will certainly discover terrestrial exoplanets, and will allow us to start studying the distribution of planet sizes and orbits down to Earth-sized bodies, but they both have their limitations in terms of minimum planet size, maximum orbital period, number of detected exoplanets and capability of further characterization of exoplanet and their host stars. Clearly, there is a need for a further generation mission that will overcome these limitations and take the next step in exoplanet detection and characterization.

Of particular importance is the precise characterization of host stars of exoplanetary systems, as discussed earlier. One of the most powerful tools for this characterization is asteroseismology, which can be used to measure the masses, radii and ages of the host stars.

Asteroseismology of a large sample of stars all across the HR diagramme can also bring us a full and deep understanding of stellar evolution, which is central to astrophysics. In particular, stars are the basic "clocks" with which we can measure ages of stellar systems within our galaxy, and thus calibrate age estimators in the Universe on larger scales. For instance, dating stellar members of the different components of galactic structure, such as bulge, halo, thin disk, thick disc, would lead to fundamental advances in our understanding of galactic structure formation and evolution.

Stars are also responsible for most of the chemical evolution of the Universe, elements being created and destroyed by nuclear burning in their deep interiors, before they are returned to the interstellar medium at the end of the stars' lives. A clear and reliable understanding of stellar evolution is therefore essential to our description of chemical evolution of galaxies and of the Universe.

A good knowledge of the evolution of cool stars is also crucial for our understanding of the past and future evolution of the sun and solar system. Finally, stellar interiors constitute laboratories for studying physical processes such as *e.g.* convection in extreme conditions that cannot be reproduced on Earth.

In the area of asteroseismology, a first important step will be taken by CoRoT, while *Kepler* will also include an asteroseismology programme, but they will both provide seismic data for only a handful of targets, and a next generation mission is clearly needed.

The basic goals of the PLATO mission are therefore:
- to open a new way in exoplanetary science, by provid-

ing a full statistical analysis of exoplanetary systems around stars that are bright and nearby enough to allow for simultaneous and/or later detailed studies of their host stars;

- to extend by a factor four the statistical analysis of exoplanetary systems initiated with *Kepler*, by surveying many more stars down to a magnitude allowing for the detection of Earth-sized planets;

- to perform seismic analysis for a very large sample of stars all across the HR diagramme, including those with detected exoplanetary systems.

Understanding the processes of star and planet evolution, by the study of stellar interiors and the distribution of planetary systems will constitute a major step for future progress in most areas of astrophysics and in the scientific and philosophical approaches towards the origin of life in the Universe. It is the cornerstone that will bring us from the first, still fairly unsystematic planet discoveries towards a systematic survey, providing a global understanding of the richness and diversity of the "Other Worlds" that populate the Universe.

2 Scientific objectives: evolution of stars and their planetary systems

2.1 Studying stars and their planets

In our conception of planetary systems, the formation and evolution of both components, stars and planets, are intricately related. Stars and planets are born together from the same parental material, and therefore share a common initial history. In particular the initial protoplanetary disc and its central stellar core have the same chemical composition and their respective angular momentum reflects the angular momentum distribution in the protostellar/protoplanetary nebula. Also, in the early phases of evolution, young stars exchange angular momentum with their accretion protoplanetary disks, which eventually evolve into planets and transfer their angular momentum to planet orbits.

Even later in the evolution, various processes occur that result in mutual interactions between the stars and their planets. The stellar radiation flux obviously impacts the planet atmospheres, while particle bombardment of the planet by the stellar winds can also affect the chemical and biological evolution of the planets. Planets can also influence their parent stars, *e.g.* by colliding with them, and enriching them in various chemical elements [20]. Giant planets in close-in orbits can also influence their star's rotation via tidal effects.

The study of planetary system evolution thus must be considered as a whole and it cannot be separated

from that of stellar evolution. We cannot understand how planets are formed and how they evolve without a proper knowledge of stellar formation and evolution. We cannot characterize planetary systems without characterizing precisely their host star. The basic philosophy behind the PLATO mission is precisely to study complete planetary systems composed of planets and their host stars, these two components being observed together with the same technique.

2.2 Evolution of planetary systems

Our understanding of planetary system formation and evolution is insufficient. Detections of giant exoplanets have revealed a large variety and complexity of configurations in exoplanetary systems, which was totally unexpected. Major questions and uncertainties remain, which hamper our progress in this area.

The true distribution of characteristics of exoplanets and of their orbits is unknown, with current knowledge strongly biased from the detectable sub-sample. In particular, we do not know the distribution of planets with sizes and masses significantly smaller than those of gaseous giant planets. The extension of our investigation of exoplanets toward lower masses, down to terrestrial planets, may reveal further surprises. The first planets with masses corresponding to Neptune have been discovered recently, but their nature still remains obscure.

A full statistical description of exoplanetary systems, down to masses and sizes of a fraction of those of the Earth, is a prerequisite for any decisive advance in the field of planetary formation and evolution. It is therefore necessary to extend significantly the sample of detected exoplanets beyond CoRoT and *Kepler*. This constitutes one of the objectives of PLATO.

A basic goal of PLATO is also to provide a large sample of exoplanets around bright stars, spanning a wide range of orbits, sizes and masses, and to measure precisely and reliably their orbital parameters, sizes, masses and ages. This requires a detailed characterization of their central stars, involving both seismic observations with PLATO and ground-based support observations, allowing us to measure all their fundamental parameters, including mass, radius, age, temperature, chemical composition, rotation. Exoplanetary transit techniques indeed give access to the ratio of planet to star radii, so that the planet sizes cannot be determined if the star radii are not perfectly known. Similarly, radial velocity techniques, even when the inclination angle is known, provide the ratio of planet to star masses, and a good measurement of the star's mass is

needed. Star radii and masses are usually estimated by locating the star in the HR diagramme, which is imprecise and often unreliable. Finally, the understanding of exoplanetary system evolution requires an estimate of their ages, which can only be obtained by a measurement of the age of their central stars.

Such an approach is beyond our capabilities for most of the planets that will be discovered by CoRoT and *Kepler*, which are orbiting stars that are too distant and too faint for such a detailed characterization, but is within reach of PLATO, which focuses on stars that are bright and nearby.

Some particular examples of investigations that require a precise characterization of exoplanets and their central stars are indicated briefly below:

- the full knowledge of the properties of planets, their orbits and their parent stars, in particular their ages, will allow us to understand the mechanisms controlling orbital eccentricities and planet migration [28].
- the investigation of the still mysterious connection between giant planets and the metallicity of their parent stars requires good statistical knowledge of planet and parent star properties, including stellar ages and metallicities, of the type PLATO will provide [37].
- the potential chemical composition difference between the inner part and the external convective zone of a star, that will be present if high metallicity hosts have ingested planetary material [5], can be investigated via asteroseismology.

2.3 Stellar evolution

Theory of stellar evolution has undergone major progress in the last decades. However, in spite of the progress in our understanding of microscopic physics in stellar interiors, our description of some physical processes controlling stellar structure and evolution is subject to major uncertainties. Convection and various other mixing and transport processes are poorly understood and yet play a major role in stellar evolution, determining evolution timescales, and must be taken into account for measuring stellar ages. Our current poor knowledge of most of these processes is usually compensated in our modeling by some poorly constrained parameterisation, and therefore the resulting stellar ages are model dependent and unreliable.

One of the consequences of this unsatisfactory modeling is that the ages of the oldest globular clusters are still very uncertain, and for some values of the model free parameters can still be higher than the estimated age of the Universe [43] [13] [22]. Additionally, the relatively large adopted value of the core overshoot-

ing parameter needed to fit young open cluster data [25] is in contradiction with recent asteroseismic estimates for this parameter for field β Cephei stars [2] [29]. This clearly points out that our current knowledge of convective and rotational mixing processes inside massive stars is very incomplete, resulting in huge uncertainties in stellar masses and ages of supernova progenitors. Uncertainties in convective overshooting can lead to uncertainties in the ages of open clusters up to a factor of two [30]. Considering these difficulties, it is clear that the age ladder of the Universe, which rests on stellar age estimates, is still highly unreliable.

Our modeling of stellar interiors and stellar evolution therefore needs to be seriously improved. The situation for the Sun has evolved considerably with the advent of helioseismology, which has provided precise insight into the properties of the solar interior [11]. Based on this very positive experience, it is clear that asteroseismic investigations, *i.e.* measurements of oscillation frequencies, amplitudes and lifetimes of a large number of stars of various masses and ages constitute the only and necessary tool to constrain efficiently our modeling of stellar interiors, and improve our understanding of stellar evolution [35].

The pioneering CoRoT space mission is bringing us essential information to progress in this area, by providing high precision asteroseismic measurements for a few dozen stars distributed in several regions of the HR diagramme. The *Kepler* mission will also include a limited asteroseismology programme. However, these first measurements will remain limited to small and strongly constrained samples, which do not contain for example members of open clusters, or old population II stars, which would constitute major targets for such investigations, as detailed below. A better and more complete exploration of seismic properties of various classes of stars, sampling all stellar parameters (mass, age, rotation, chemical composition) is necessary. Such is the goal of PLATO.

2.4 Detection and characterization of planetary transits

Planetary transits can be detected through high precision photometric monitoring, as illustrated by Figure 1. A planetary transit in front of a stellar disc causes a decrease of the photometric signal $d = (R_p/R_*)^2$, where R_p and R_* are the radius of the planet and of the star, respectively. For a star like the Sun, the typical relative variations are 10^{-4} , with 13 hour duration for 1 AU orbits, for Earth-size planets, and 10^{-2} for Jupiter-size bodies. Observations of recurring plane-

tary transits can be used to measure the orbital period P , and therefore the semi-major axis of the orbit, by applying Kepler’s third law.

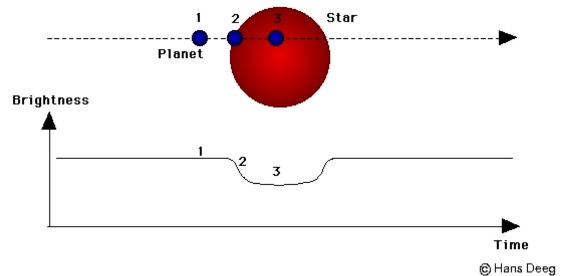


Figure 1: Schematic illustration of the dynamics of a planetary transit and the corresponding light curve.

The photometric method has the unique ability to determine the ratio of planet to star radius from the transit’s depth. It also has the potential to detect small, Earth-sized planets, and is not limited to slowly rotating stars, like the radial velocity technique.

Figure 2 clearly shows that the search for terrestrial-size planets (especially those in the habitable zone) is the unique domain of space-based photometry: (space-based) astrometry can tackle higher-mass, longer-period planets, while the radial velocity searches excel for the shorter-period giant planets.

The main objective of PLATO for exoplanetary science being to detect planets of all sizes, around all types of stars, and to characterize them completely, transit observations therefore constitute the best and the most unbiased technique.

Besides the direct detection of planetary transits and the measurement of planet sizes, orbital periods and semi-major axis, high precision photometric observations obtained by PLATO will result in the measurement of other critical physical characteristics of extra-solar planets:

Albedo of close-in planets and detection of stellar reflected light: the albedo is one of the key surface properties of a planet. Accurate photometry will allow the measurement of the albedo of the close-in planets, of which large numbers will be found by PLATO. The fraction of reflected stellar light by a close-in giant exoplanet depends linearly on its albedo A , and the flux variation due to the modulation of the reflected light along the planet orbit is typically $\Delta F_*/F_* \approx 0.25 \times 10^{-4} A$, for a planet orbiting at ≈ 0.05 AU from its host star [39] [40]. Because the monitoring of such targets will cover several hundred planet orbital periods, such a modulation will be detectable by PLATO

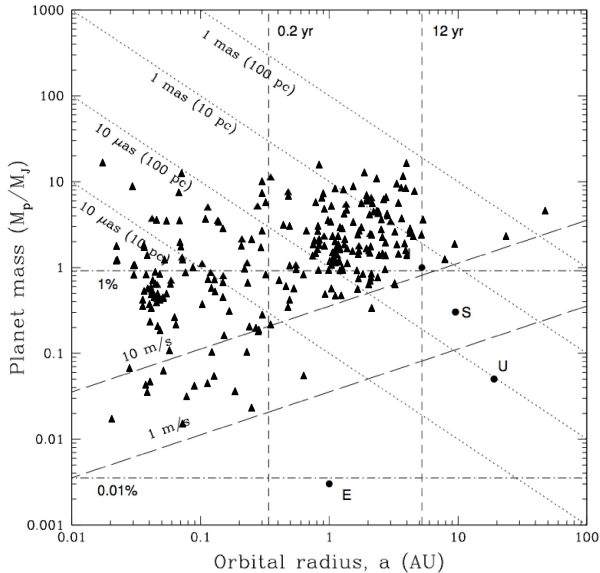


Figure 2: The capabilities of planetary search methods, shown in the orbital period versus planetary mass domain. dots: solar-system planets; triangles: extra-solar planets discovered up to now; dotted lines: astrometric searches; dashed lines: radial velocity searches; horizontal dashed-dotted lines: photometric transit searches. As can be seen, *individual transits* from Earths can be detected with accurate (10^{-4}) photometric searches (the type of data PLATO will naturally produce), while they are inaccessible for either of the other methods.

down to $m_V=9-10$ for albedos as small as $A = 0.3$.

High precision photometric monitoring will therefore allow us to detect giant exoplanets in close-in orbits around stars down to $m_V=9-10$, *even* for large inclination angles, where occultations are not visible.

Physics of planet interiors: as discussed below, follow-up ground-based radial velocity measurements will be used to determine the mass of a large fraction of the detected planets (the inclination, which enters in the mass determined by radial velocity through the $\sin i$ factor, being accurately constrained by the presence of transits). The transit depth will measure the ratio of the planet radius to the star radius, and the star radius will be well determined by the seismology measurements. The planet radius will therefore be derived with great accuracy, and we will have a direct measure of the mean density, and thus constraints on the internal structure of the planet.

Astrometric detection of planets: the star reflex motion induced by planet revolution, which can be measured by accurate radial velocity monitoring, also creates an astrometric wobble, which can be expressed as $w = 3 \times a/d \times m_{pl}/M_*$, where w is the amplitude of the astrometric wobble in μas , a is the semi-major axis of the exoplanet orbit in AU, m_{pl} and M_* the mass of the planet and its star (expressed in m_{Earth} and M_{\odot} , respectively), and d the distance to the exoplanetary

system in pc. Thus a $1M_J$ exoplanet, orbiting a $1 M_{\odot}$ star at 1 AU, placed at 15 pc, so that the star has $m_V=6$, would induce a $60 \mu\text{as}$ wobble.

If we measure the astrometric position of each star in the surveyed field relative to all other stars in the field, and if the astrometric measurement is limited by photon noise, precisions of about $6 \mu\text{as}$ may be achieved down to $m_V=6$ after one month of integration. This will be amply sufficient to detect all giant exoplanets with orbits near 1 AU, orbiting nearby bright stars, irrespective of the inclination angle of the orbital plane with respect to the line of sight.

These astrometric measurements, coupled with measurements of reflected stellar light described earlier, will constitute a powerful tool for identifying exoplanetary systems around nearby stars, out to distances of 15–20 pc, and therefore can help select targets for future interferometric and coronagraphic missions.

Satellites and rings: high precision measurements of planetary transits can be used to detect the presence of satellites and rings of the observed exoplanets. The presence of planetary rings affects the shape and duration of the planetary transits: for a Saturn-like planet at one AU from the parent star, the ingress and egress take one hour for the planet and two hours for the ring. In addition, the planet ingress (egress) starts (ends) steeper for the planet than for the ring. Finally, the projected inclination of the ring with respect to the planet’s orbital plane and the ring optical depth can be derived from the transit shape [38].

Satellites of the observed exoplanets can be detected directly by the shape of the transit curve if they are sufficiently large, or by their perturbation of the transit timing of their parent planet (see below).

Timing detection of satellites and of further planets: in a system with a known transiting planet, further bodies will cause small distortions to the transiting planet’s orbit. These distortions manifest themselves in deviations of the transits from strict periodicity; and will be measurable in data with sufficient signal and temporal resolution. Such timing measurements can be applied to the detection of satellites around transiting planets [41]. For example, Saturn’s moon Titan would cause transit timing variations of Saturn with an amplitude of 30 seconds, whose detection would be within the capabilities of PLATO. Additional non-transiting planets could be detected as well [1] by their influence on the barycenter of the star - transiting planet system, and current ground-based observations are already being analyzed for the presence of such further planets [15].

2.5 Asteroseismology

Oscillating stars can be found almost everywhere in the HR diagramme (Figure 3). Measurement of a set of oscillation frequencies enables us to infer their internal structure and hence state of evolution. Each frequency senses a different weighted function of the stellar interior. A set of frequencies can yield detailed knowledge of the internal structure, enabling us to deduce the state of evolution and hence the age.

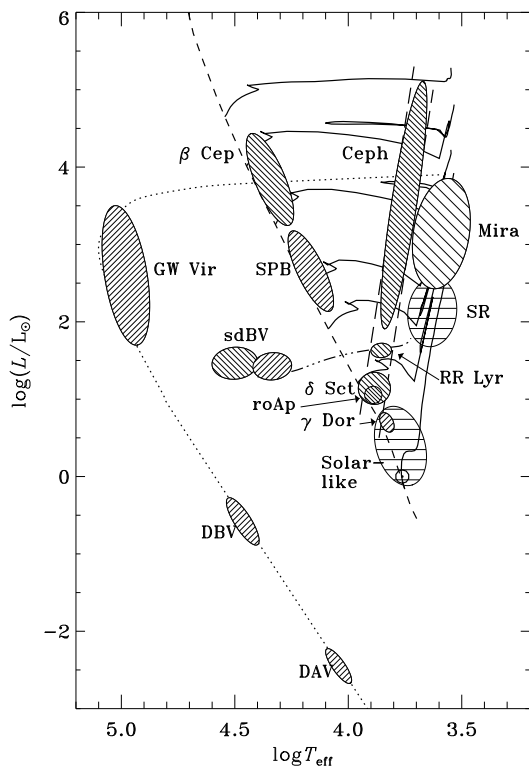


Figure 3: Schematic location of various classes of pulsating stars in the Hertzsprung-Russell diagram. The solid lines show evolutionary tracks for stars of masses (from the top) of 20, 12, 7, 4, 3, 2 and 1 solar masses.

The power of such analyses has been forcefully demonstrated in the solar case, where helioseismology has provided dramatic insight into the properties of the solar interior. Through inversion of extensive sets of frequencies it has been possible to determine the sound speed in most of the Sun, hence testing in detail models of solar structure. This has revealed anomalies below the outer convective zone and just outside the solar core, and also allowed investigation of subtle features of the thermodynamic properties of matter in the Sun, as well as a precise determination of the solar envelope helium abundance. The general agreement between the inferred structure of the solar core and normal solar models strongly indicates that the solution

to the solar neutrino problem must result from previously unsuspected properties of the neutrinos, rather than deficiencies in the solar models. Analyses of frequency splittings have yielded detailed determinations of the internal angular velocity. Many of these results are based on the excellent observations obtained from the ESA/NASA *SOHO* mission.

In contrast to helioseismology, seismology of distant stars is restricted to low-degree modes, but it is just these modes that penetrate into the deep interior and therefore convey information on the interior structure and state of evolution. Furthermore, the comparatively limited set of modes accessible in stars is compensated by the richness of stellar properties that may be investigated, far beyond the properties of the solar interior, such as the mass and radii of convective cores, rapid rotation and the variation with mass and chemical composition. This will, for example, allow detailed investigations of the uncertain mixing processes associated with convective cores in main-sequence stars, of great importance to their subsequent evolution.

Members of *open clusters* present a specific interest. Their uniform chemical composition and age, and nearly common distance, provide very stringent constraints on the modeling, increasing the information obtained from the oscillation frequencies. In young clusters, we may in particular observe the β Cephei stars, and bring important constraints on the evolution of massive stars. In the older clusters, oscillations in sub-giants (similar to those observed in η Bootis [9]) can be studied. Therefore, the asteroseismic analysis of members of open clusters chosen to sample an age sequence, will allow us to constrain severely stellar evolution modeling.

Also, the properties of the metal-poor stars (Pop. II stars) are of great interest; these are expected to be amongst the oldest in the Galaxy, often similar to the stars that are used for age determinations of globular clusters, and may provide important limits on the age of the Galaxy and, by implication, the Universe.

The modes of oscillation can be conveniently represented in terms of surface harmonics $Y_{\ell m}$, radial eigenfunctions $\xi_{n\ell m}$ and oscillation frequencies $\nu_{n\ell m}$ where n is the order of the mode (approximately the number of nodes in the radial direction), and ℓ is the degree, determining the overall horizontal scale. For a spherical star the azimuthal order m is degenerate, the degeneracy being lifted by a non-radial perturbation, *e.g.* rotation. A typical mode is represented in Figure 4.

The relation between the frequencies and the internal properties of the star is reasonably well understood; based on this understanding one can isolate informa-

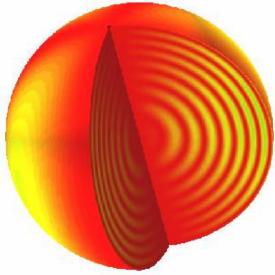


Figure 4: Example of a non-radial oscillation mode with $\ell = 2$, $m = 2$, $n = 18$. This simulation of the pulsating star illustrates the surface behaviour of the mode, determined by the relevant spherical harmonic, as well as the behaviour in the interior which is shown in the cut-out. Note that the amplitude is substantial even in the central region of the star, reflecting the sensitivity of the oscillation frequencies to the core structure.

tion about particular properties of the star, or regions within it, by suitably combining the frequencies.

Low-degree acoustic modes accessible for distant stars probe their central regions. Even more sensitive probes of the core are obtained where g modes can be observed. Important goals of the analysis are evidently to determine the overall parameters of the stars. In particular, the stellar ages, particularly important in the framework of PLATO, since their measurement will allow us to estimate the ages of the detected planets, can be determined as a result of the sensitivity of the frequencies to the structure of stellar cores. At a more fundamental level, the asteroseismic data can be used to investigate the complex physics that determine stellar structure and evolution; this will not only improve the calculations of stellar models but will also enable us to utilize the observations to learn about physics of matter under extreme conditions.

The oscillation frequencies of a star exhibit some regular patterns which allow diagnostic information on specific characteristics of the stellar structure to be derived, even in the presence of low S/N data. This regularity can be clearly seen in the solar spectrum shown in Figure 5: the main characteristic of this spectrum is the approximately equal “large separation” ($\Delta\nu_\ell$) of $\approx 135 \mu\text{Hz}$ between the larger peaks corresponding to p modes with (n, ℓ) and $(n - 1, \ell)$, but important information is also encoded in the “small separation” ($\delta\nu_\ell$) between peaks with nearly the same frequency corresponding to p modes with (n, ℓ) and $(n - 1, \ell + 2)$.

These two numbers alone give significant constraints. The average large separation Δ contains information on the mean properties of the star, *e.g.* its mean density, while the average small separation δ is

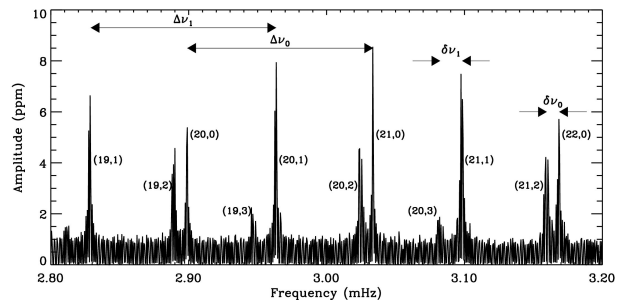


Figure 5: Amplitude spectra of solar oscillations measured in intensity by the VIRGO instrument on the *SOHO* spacecraft. The figure shows only a portion of the solar oscillation spectrum, illustrating the details of the definition of the “large” and “small separations”. Each frequency peak is labelled with the n, ℓ values of the oscillation mode.

sensitive to the chemical composition in the central regions, and can therefore measure the central hydrogen content, hence the age of the star.

In addition to the simple use of the asymptotic behaviour of stellar oscillations described by the large and small separation, a complete inversion of all measured mode frequencies can be performed to determine the internal structure of stars. Such inversion techniques have been developed and successfully applied in terrestrial and solar seismology where the measured set of frequencies span a large range of n, ℓ values. New techniques have been developed which are applicable to data sets with only low ℓ values – such as would be obtained with PLATO. These techniques have been extensively described in the recent literature, and are not discussed in detail here.

Rotation removes the m degeneracy in the frequencies; the resulting m -dependence of the frequencies permits the determination of the internal angular velocity $\Omega(r)$ inside the star, as a function of r . The measurement of the so-called *rotational splitting*, *i.e.* the difference between frequencies with the same n, ℓ but different m , for different values of n , can be used to infer the internal rotation rate and its variation with radius. An example of what can be achieved is presented in [24], who considered a model of an evolved $1.5 M_\odot$ star with a prescribed $\Omega(r)$ and a surface rotational velocity of 30 km s^{-1} , and showed that inversion of the frequency splittings for an assumed rotation profile reproduced the input rotation profile to excellent accuracy, with frequency measurement accuracies typical of what is expected from CoRoT, ranging from 0.05 to $0.22 \mu\text{Hz}$, depending on the mode lifetime.

2.6 Follow-up observations

A vast ground-based programme, in particular to identify real planets from transit candidates, will be an integral part of the overall mission, and will be organized should the mission be selected. Indeed radial velocity observations, as well as ground-based imaging and photometry observations are required in complement to the space photometric data, obtained with wide PSFs. The ultra-precise photometric observations provided by PLATO will also need to be complemented by ground- and space-based follow-up observations, in order to complete the characterization of the detected planetary systems, their central stars, as well as all the stars in the PLATO programme. One of the main advantages of the approach proposed for PLATO will be to focus on bright stars, so that this follow-up will be made easy and efficient.

We give below some relevant examples of follow-up observations that will be needed.

Radial velocity measurements: a radial velocity monitoring of the stars with planetary transit candidates detected by PLATO will be necessary in order *i)* to confirm when needed that the candidate transit was indeed produced by a planet, and *ii)* to provide a measurement of the planet mass, taking advantage of the accurate knowledge of the star’s mass derived from seismic analysis with PLATO. Today’s state-of-the-art radial velocity monitoring, such as performed with the HARPS spectrograph at the ESO 3.6 m, can reach precisions of the order of 1 m s^{-1} , sufficient to detect the signature of planets with a few Earth masses around solar-type stars [42]. As argued in Section 2.9, we cannot reasonably hope to lower significantly this detection limit. However, although PLATO will detect many smaller and less massive planets, the planet mass measurements down to a few Earth masses will be crucial for the characterization of a large fraction of the planet sample detected by PLATO. Note that very high resolution and very stable spectrographs, of the same type as HARPS at the ESO 3.6 m, will certainly be available at the time the first Cosmic Vision M mission is flown, and later. For instance, one of the main instruments foreseen for the e-ELT, CODEX, is precisely of this type.

Differential photometry and spectroscopy: planets around bright ($m_V = 4\text{--}10$) stars detected with PLATO will have a long-lasting legacy for future follow-up observations to characterize further the nature of extrasolar planets. Photometric and spectroscopic observations of the upper atmosphere levels can be obtained during primary and secondary eclipse of

the planets orbiting nearby and bright stars, which are observable at very high signal-to-noise ratio. Several transiting planets in the recent past have already shown the huge potential of such characterizing observations and their impact on our understanding of the formation and evolution of planets. Thermal emission of HD189733b, HD149026b, HD209458b and TrES-1 [21] [18] [14] [31] [44] has been detected with the Spitzer infrared telescope. Infrared spectra of HD189733b ($m_V = 7.7$ [18]) obtained with Spitzer provided upper limits on water and methane absorption. TrES-1 ($m_V = 11.8$) observations gave upper limits on CO and water. The best characterized planet so far is HD209458b ($m_V = 7.7$). In this planet water and silicate clouds [31] have been detected in the infrared with Spitzer, sodium absorption [10] in the optical and HI, OI, and CII [44] in the UV by HST. Future detections of planets around bright stars with PLATO are expected to provide "gold-mine" of targets for further planet characterization. At the time the first M-class Cosmic Vision mission will be flown, several very efficient space- and ground-based facilities will be available for these purposes, including JWST for infrared photometry and spectroscopy, and the e-ELT for high resolution spectroscopy in the optical and near IR.

High resolution spectroscopy: all stars observed by PLATO will be easily observable in high resolution spectroscopy in the optical and near IR, with various instruments on 4- and 8-m class telescopes (*e.g.* the VLT). Such observations will be used both in preparation and as follow-up of PLATO, for deriving all fundamental parameters of stars, such as their effective temperature, surface gravity, surface chemical composition, rotation velocity, level of magnetic activity, etc. Such information will be essential, in addition to the asteroseismic parameters derived from PLATO photometry, for refining the modeling of these stars.

Gaia: among the various complementary observations for PLATO, those provided by *Gaia* will play a particularly important role. The precise parallaxes derived by *Gaia* for all stars observed by PLATO will be used to measure their absolute luminosities and place them accurately on the HR diagramme. Also, coupled with interferometric measurements of stellar angular diameters for the most nearby of these stars, these precise parallaxes will give us an independent measurement of the physical diameter of these stars, a very powerful additional constraint for their modeling.

Ground-based interferometry: angular diameters of stars out to several tens of parsecs are within reach of present and future ground-based interferometers, such as VLTI. In some cases, these interferometric observa-

tions may also be used to directly detect and characterize giant exoplanets around nearby stars, in particular those that will have been identified by PLATO.

Space interferometry: finally, future interferometric missions, can use PLATO results to identify the best targets for studying terrestrial planets and their atmospheres. The number of bright and nearby stars monitored by PLATO is high enough that we can hope to detect a couple of transiting terrestrial planets around very bright stars, and in any case PLATO will discover a significant number of giant exoplanets around these nearby stars, either by the reflected stellar light on the planet atmosphere, or by the astrometric measurement of the star’s reflex motion.

2.7 Additional science

The PLATO mission can be used for other purposes than the primary science goals and many targets not directly related to such goals will be automatically observed simultaneously. As a consequence, fascinating possibilities for additional science projects emerge. In the following we highlight some of the additional science potential of PLATO and are sure that more will emerge while developing this mission. MOST and CoRoT [45] have clearly confirmed the extremely attractive additional science potential of ultra-high precision photometric missions and *Kepler* certainly will provide a further proof.

Kuiper Belt objects, exo-comet transits: the discovery of hundreds of transneptunian objects has confirmed the hypothesis of a residual protoplanetary disc beyond Neptune, a key element to reconstruct the history of the Solar System. Serendipitous stellar occultations are a powerful tool to detect these small objects orbiting beyond Neptune [34]. PLATO could allow the detection of very small objects and constrain their size distribution. In addition, an important by-product of the transit search could be the detection of exo-comets.

Pre-main-sequence stars: high precision photometric monitoring of the PMS T Tauri and Herbig Ae/Be stars will provide information on phenomena linked to accretion onto the surface of these stars; in particular, PLATO will provide valuable information on periodic phenomena, such as rotational modulation due to hot/cold spots on the stellar surface, or non-periodic phenomena, like accretion events and flares.

Stellar activity and flares: studying with PLATO the brightness variations on time scales of days to months will allow us to detect small solar-like spots, derive the lifetimes of surface features, hence to estimate the turbulent magnetic diffusivity in the upper layers of the

convection zones [33], and to measure rotation and stellar differential rotation, which is fundamental to test the available hydromagnetic dynamo models. Finally, the monitoring of dMe flare stars will shed some light on the mechanisms of coronal heating by investigating the statistics of white-light stellar micro/nano-flares and related precursor phenomena.

Stellar rotation: the measurement of rotation rates for a vast sample of stars, as well as the measurement of their ages via asteroseismology, will allow a full calibration of the rotation period–age relationship, providing important tests of stellar dynamo models. Furthermore, following the evolution of rotationally modulated light curves over many rotation cycles will allow investigating differential rotation, as has been successfully demonstrated by MOST [36][12].

Cataclysmic variables: the cataclysmic variables (CVs) are binary systems consisting of an accreting white dwarf (WD) and a late type secondary star filling its Roche lobe. Depending on the strength of the magnetic field, matter accretes onto the WD via a disk or directly channeled towards the magnetic poles. Hence CVs represent close-by test objects of accretion processes in different physical environments. High precision photometric monitoring of CVs can be used to study these accretion phenomena; the periodic light variations are related to the binary system, while non-periodic variations are due to mass accretion changes or instabilities in the accretion disc or accretion flow.

Only a few examples of additional science programmes are briefly mentioned above. Obviously many other scientific investigations can be carried out with the help of the huge database of ultra-high precision photometric monitoring provided by PLATO.

2.8 Required observations

2.8.1 Basic observation strategy

The PLATO science objectives can be met using long uninterrupted high precision photometric monitoring of large samples of stars. These observations will first allow us to detect and characterize planetary transits, allowing us to measure planet sizes and orbital periods, as well as to detect planet satellites and rings. They will provide us as well with measurements of frequencies, amplitudes and lifetimes of oscillation modes of the same sample of stars. The analysis of these asteroseismic measurements will yield precise information about the internal structure and rotation of these stars, and in particular will allow to determine accurately their masses, radii and ages.

2.8.2 The stellar sample

A first sample of PLATO targets will contain objects that are bright enough to reach photometric precision allowing us to use seismic tools and also to perform efficient ground-based follow-up, and still numerous enough to allow for a large number of planetary transit detections in spite of the low geometrical probability that the line of sight is favourably oriented with respect to the planet orbital plane. This geometrical probability is typically of the order of 1% for Sun-Earth analogs. As demonstrated *e.g.* in the framework of the CoRoT, *Eddington*, *Kepler* missions, a prerequisite for such observations is to survey a sample of about 100,000 stars, out of which about one half will be cool dwarfs, adequate for transit search programmes.

A scaling up of preliminary results of CoRoT shows that reasonably sized optical monitors, typically with one square meter collecting area, are capable of detecting and exploiting solar-like oscillations down to $m_V = 11 - 12$. Such objects will also be efficiently observed from the ground in high resolution spectroscopy.

Therefore, the primary stellar sample for PLATO will be a set of at least 100,000 stars brighter than $m_V = 11 - 12$, observed at ultra-high precision.

In addition to this main sample, for which both transit search and asteroseismology will be performed, an extended sample of fainter stars needs to be observed, in order to extend the statistical analysis of exoplanetary transits. This second sample will include about 400,000 additional stars down to $m_V = 14$, which will be observed to a sufficient precision to detect the transits of Earth-sized planets.

Moreover, as mentioned earlier, asteroseismic observations of stars that are members of open clusters, chosen to offer a complete sequence of ages, as well as old population II stars, will be of major interest, and such targets should definitely be included in the programme.

2.8.3 Surveyed field

We have examined existing stellar catalogues, in particular the 2MASS and USNO catalogues, in order to estimate the minimum field of view to survey to comply with the stellar sample requirements. Several regions were explored in the vicinity of the galactic plane. We find that the sky is very inhomogeneous at $m_V = 11 - 12$, so that the field(s) to be monitored must be chosen with care. Typically, the most populated fields seem to be in the southern hemisphere. As an example, Table 1 indicates the total number of stars counted from the 2MASS catalogue, down to $m_V = 11, 11.5$, and 12 in one such typical field. An estimate of the number

of stars down to $m_V = 14$ is also given, based on star counts from the USNO-B1 catalogue in several smaller regions within the same field.

From these star counts, we conclude that the minimum required field would be of 20° diameter, *i.e.* about 300 square degrees.

2.8.4 Photometric noise level

The depth of a planetary transit is given by the ratio of the areas of the planet and its transited star, which is of the order of $\Delta F_*/F_* \simeq 10^{-4}$ in the case of Sun-Earth analogs, while transit durations are typically of the order of 12 hours. In order to detect such transits at more than 4σ , a dimensioning requirement, we need to obtain a photometric noise level lower than about 2.5×10^{-5} in 12 hours, *i.e.* about 8×10^{-5} in one hour. However, this requirement must be considered as the minimum one, since the detection of planets with sizes smaller than the Earth's, the detection of Earth-sized planets in front of stars hotter than the Sun, and the measurement of several points across the transits would be of major interest. We will set as a goal specification a photometric noise level of 2.5×10^{-5} in one hour, allowing us for instance to measure about ten points across the transits, and therefore to characterize them with high reliability and precision. Such a low noise level would also allow us to detect Earth-sized planets in front of $2 R_\odot$ stars, which are in principle less active and therefore less intrinsically variable than solar twins, so that the detection of such exoplanets may in fact be easier than for solar-Earth twin systems; we would therefore extend to hotter stars the statistics of terrestrial exoplanets.

Figure 6 shows simulated light curves with various levels of noise, all including a 12 hour transit with a depth of 10^{-4} , illustrating the absolute need for a noise level better than 8×10^{-5} in one hour for detecting such a transit and the potential for precise transit characterization at a noise level of 2.5×10^{-5} in one hour.

The dimensioning requirement for seismic investigations is to detect and characterize oscillations of solar-type stars, which are the lowest amplitude oscillators. Ground-based spectroscopic observations have recently revealed solar-like oscillations for a handful of bright stars, whose amplitudes, when translated in terms of photometric variations, range from a few ppm to a few tens of ppm [19]. These conclusions have been recently confirmed by preliminary results from CoRoT.

The corresponding requirements on the photometric noise require that we should be able to detect individual p -mode oscillations in cool dwarf stars as faint as

field diameter	$N(m_V \leq 11)$	$N(m_V \leq 11.5)$	$N(m_V \leq 12)$	$N(m_V \leq 14)$
30°	60,000	132,000	280,000	2,200,000
	25,000	53,000	115,000	890,000
20°	32,000	73,000	125,000	890,000
	13,000	29,000	50,000	360,000

Table 1: Number of stars counted in fields centered at ecliptic coordinates (210°, -60°). The first row gives the total number of stars, while the second row indicates an estimate of the number of cool dwarfs, calculated using the fraction of cool dwarfs from the Besançon model [32].

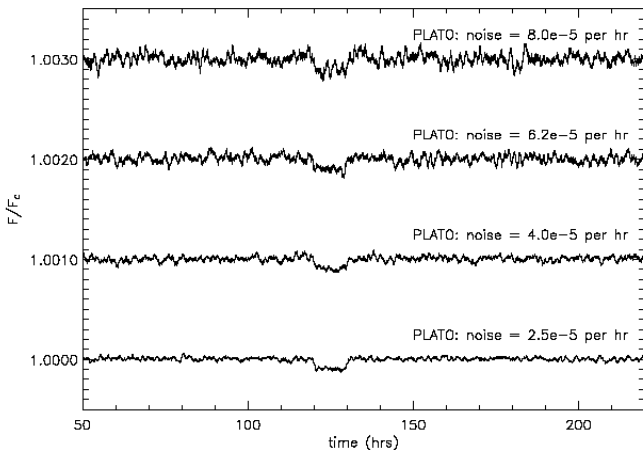


Figure 6: Simulated light curves assuming various noise levels, and including one single transit with a depth of 10^{-4} and a duration of 12 hours. With a noise level of 2.5×10^{-5} in one hour, the transit is seen with no ambiguity and can be characterized, even at its first occurrence; the reliability of detection and characterization decreases with increasing noise level. A noise of 8×10^{-5} in one hour is the maximum acceptable for a transit detection at first occurrence.

$m_V = 11$. This means that the total photometric noise in the observations must remain below $\simeq 1$ ppm after approximately 30 days of observation, down to $m_V = 11-12$, in the whole frequency range of interest, *i.e.* from 0.1 to 10 mHz. Figure 7 shows a portion of the simulated power spectrum for a $1.2 M_\odot$ star observed for 50 days with such a photometric noise, as well as that expected for brighter stars leading to lower noise levels. The spectrum was generated with a simulator built in preparation for CoRoT, including photon noise and stellar granulation noise, and its results have been successfully compared to the early results of CoRoT.

The noise levels requirements of 2.5×10^{-5} in one hour and one ppm in 30 days are very similar. These photometric noise requirements impose that *i)* the photon flux of the target stars is sufficiently high to ensure that photon noise complies with the final noise specifications, and *ii)* that all other sources of noise remain well below photon noise in the frequency range of interest. The required photon fluxes can be translated into requirements on optics collecting area and overall

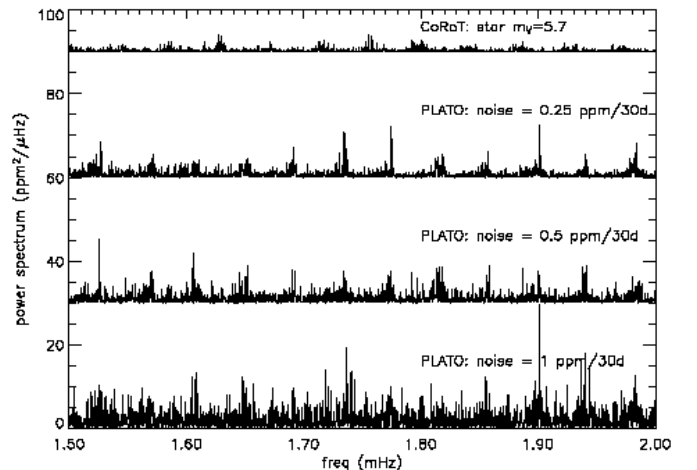


Figure 7: Expected power spectrum for a $1.2 M_\odot$ star, observed for 50 days, with a noise level of one ppm in 30 days (lower curve). Such a noise level will typically be obtained at $m_V=11.5$ or 12 with PLATO, depending on the details of the instrumental design. The next two curves correspond to better noise levels of 0.5 and 0.25 ppm in 30 days, achievable with PLATO at $m_V=10$ and 8.5, respectively. Note that the oscillation spectrum, clearly visible at low noise levels, is only barely visible on the lower one, indicating that one ppm in 30 days is indeed the upper limit for the specified noise level. The upper curve shows a preliminary result obtained with CoRoT in 50 days on a solar-type star with $m_V=5.7$, which translates to $m_V=8.5$ for PLATO when the ratio of collecting areas is taken into account. This CoRoT result demonstrates that the noise levels introduced in the simulation are realistic and that solar-like oscillations can indeed be easily observed in photometry from space.

throughput described in the following section.

2.8.5 Collecting area and overall throughput

The above noise requirements, applied for stars with $m_V = 11-12$, imply a photo-electron flux of the order $4 \times 10^5 \text{ sec}^{-1}$ at this magnitude, which requires the use of an optical design with a high overall throughput and a large effective collective area.

The overall optics + detector throughput can reasonably be expected of the order of 0.6 in average over a bandpass of 500 nm, using high quantum efficiency detectors, such as, *e.g.*, thinned backside illuminated CCDs, as well as efficient, optimally coated optics. Under these assumptions, it can be calculated that an ef-

fective total collecting area of 0.8 m^2 is necessary to yield the required photo-electron flux down to $m_V = 12$, while a collecting area of 0.7 m^2 would comply with the flux requirement at $m_V = 11.5$

2.8.6 Non photonic sources of noise

We must ensure that additional sources of noise remain significantly below photon noise. Until a full analysis of all environmental and instrumental perturbations is carried out, we will specify that any given source of noise must remain at least three times below photon noise for stars in our prime sample of stars, *i.e.* down to $m_V = 11 - 12$. We provide below some hints concerning the expected two major sources of perturbations, satellite jitter and thermal instability, but a thorough study of all possible other sources of noise must be carried out when designing the instrument and the mission during assessment, phase-A and B1.

Satellite jitter introduces photometric noise, as drifts in the star's position will change the illumination pattern of the detector, whose pixels do not have exactly the same sensitivity. While a large fraction of the induced noise can be calibrated out, as demonstrated by CoRoT results, a residual noise will still be present, and impose pointing stability requirements. At $m_V = 11 - 12$, the photon noise will be of the order of 2×10^{-4} per minute, and jitter noise must remain about three times below this value, *i.e.* below 6×10^{-5} per minute. A detailed study, depending on the instrument design, is necessary to figure out how this requirement translates into pointing stability specifications, but order of magnitude estimates, as well as experience gained with previous missions such as CoRoT, indicate that a pointing stability of about $0.2 - 0.4''$ on timescales of minutes will be needed.

Variation in temperature of both the telescopes and the CCD detectors will lead, directly or indirectly, to changes in the apparent signal level from the target stars. The top level requirement for these perturbations is that the equivalent noise level induced by thermal changes must be three times below the photon noise level across the magnitude range of interest. While detailed *a posteriori* corrections can drastically improve the resulting noise, as demonstrated by CoRoT preliminary results, a full study taking into account the details of the instrument design and environmental perturbations must be carried out in order to specify clearly the thermal stability requirements. Again, as a first estimate, we can take advantage of the CoRoT experience, and require that the chip temperature must be stable to 0.1 K/hr , while a thermal

stability of a few tenths of a K per day will be required for the telescope structure.

2.8.7 Duration of observations

The duration of the observations needs to be longer than three years, so that at least three consecutive transits for Sun-Earth analogs can be detected during the mission lifetime. A goal specification for the duration should be four years, allowing us to detect planets in more distant orbits than the Earth's and also increasing the transit detection probability.

For the seismic analysis of the target stars, the total monitoring time must be sufficient to yield a relative precision of 10^{-4} for the measurement of individual mode frequencies, which is needed to perform the inversion of the oscillation spectra. For solar-type stars, this comes down to an absolute precision of $0.3 \mu\text{Hz}$, which translates into a minimum monitoring time of one month for a reasonable S/N of 10 in the power spectrum, as can be derived from the computations presented in [23]. For red giants, which have typically frequencies of a factor 30 lower, this requirement becomes several months. The complete range of kappa-driven p and g modes in stars along the main sequence covers mode periods from a few minutes to several days, and the latter also require several months of monitoring. This is why CoRoT performs 5-month monitoring runs. Therefore, a monitoring time of a few months is required for the seismic analysis of the programme stars, the minimum amount of time for target monitoring being one month.

2.8.8 Duty cycle

The probability that N transits of the same planet are observed is given by $p_N = (d_f)^N$, where d_f is the fractional duty cycle of the instrument. In order to achieve an 80% probability that all transits of a three-transit sequence are observed, a duty cycle of 93% is needed, ignoring gaps that are much shorter than individual transits. The requirement for planet-finding is therefore that gaps which are longer than a few tens of minutes do not occur over more than 7% of the time, with a loss by gaps as small as 5% being desirable.

A similar requirement is also imposed for seismology. Gaps in the data produce sidelobes in the power spectrum, which make mode identification ambiguous. Periodic gaps in the data must be minimized, as they will produce the most severe sidelobes in the power spectra. It can be shown that periodic outages representing 5% of the total time produce aliases with a power of about 1.5% of that of the real signal. Such sidelobes

are just acceptable, as they will remain within the noise for most of the stars observed. It is therefore required that periodic data gaps are below 5%.

Non-periodic interruptions have a less catastrophic influence on the power spectrum, and can therefore be tolerated at a higher level, provided the time lost is compensated by a longer elapsed time for the observation. Random gaps in the data representing a total of 10% of the monitoring time yield sidelobes with a power lower than 1% of that of the real signal, which will be adequate for this mission. The requirement on random data gaps is therefore that they do not exceed 10% of the elapsed time.

2.8.9 Coloured information

Intrinsic stellar variability due to activity or other stellar phenomena can lead to variations of the light curves that are similar to those produced by the transits of terrestrial exoplanets. Planet occultations can be discriminated from these intrinsic variations if several successive transits can be observed. In practice, planetary transits are definitely discriminated from intrinsic stellar variations only after three transits, so that the longest orbital period detectable is in average between one third and one half of the total monitoring time.

Light curves in several colours can improve significantly the situation. Planetary transits indeed are achromatic, while all intrinsic variability pattern show some degree of chromatism. Comparing the depths and shapes of the candidate transits in several colours will allow us to distinguish transits from stellar intrinsic variations. Similarly, colour information will allow to discriminate against false positives arising from of stellar configurations involving eclipsing binaries [8], whose vast majority generates a chromatic signal. The level of confidence for candidate transits will therefore be greatly enhanced at first occurrence, hence increasing significantly the range of reachable orbital periods.

In addition to the measurement of oscillation frequencies, asteroseismology requires the identification (ℓ, m) of the detected modes. Knowing the ℓ identification for the dominant modes of each of the 100,000 bright target stars of PLATO implies a significant reduction of the free parameter space of stellar models and is a requirement to guarantee successful seismic inference of their interior structure parameters and ages.

For oscillations in the asymptotic frequency regime, the derivation of frequency spacings suffices to identify the modes, as seen in the solar case in Figure 5. For most main-sequence stars excited by the κ -mechanism, when the modes do not follow particular frequency pat-

terns, the identification of ℓ can be achieved by exploiting the difference in amplitude and phase of the mode at different wavelengths [16].

However, whatever the interest of coloured information, we must not compromise photon noise, which is the most important requirement of this mission. The option to measure light curves in several colours must be brought at negligible cost in terms of photon loss. This is why the instrumental concepts presented later envisage to use dispersive elements rather than filters to produce light curves in three colours, in a similar way as what is done with CoRoT.

2.8.10 Time sampling

The duration Δt_{tr} of a transit of a planet with semi-major axis a and orbital period P in front of a star with radius R_* is given by $\Delta t_{\text{tr}} = P R_* / (a\pi)$. For true Earth analogs $\Delta t_{\text{tr}} = 13$ hours. More generally, the duration of a transit around a single star may last from about two hours (a “hot giant” planet around a low-mass star) to over one day, for planets on Jupiter-like orbits (five AU distance). Planets in the habitable zone, however, will cause transits lasting between five hours (around M stars) and 15 hours (for F stars), for equatorial transits.

Because individual transits have durations ≥ 2 hours, a time sampling of about 10–15 minutes is in principle sufficient to detect all types of transits, as well as to measure transit duration and period. However, a higher time resolution is needed in order to accurately time ingress and egress of the planet transits for which the S/N in the light curve will be sufficient. The accurate timing will allow the detection of third bodies, which cause offsets in transit times of a few seconds to about a minute, and will allow to solve ambiguities among possible transit configurations through the determination of ingress and egress time of the planet. In practice, a time sampling of about 30 sec will be necessary to analyse in such detail the detected transits.

The needed time sampling for the asteroseismology objectives can be derived directly from the frequency interval we need to explore, which is from 0.1 to 10 mHz. In order to reach 10 mHz, the time sampling must be at least twice this frequency, *i.e.* of the order of 50 sec. However, the necessary sampling will strongly depend on the type of stars considered. A sampling of about ten minutes will be sufficient for most stars in the upper HR diagramme, such as γ Dor, δ Sct, β Cep, SPB (see Figure 3), while a sampling better than 50 sec will be required for solar-type stars.

In summary, a 30 sec sampling will be needed for the cool stars in the bright sample of 100,000 stars for precise transit analysis and asteroseismology, while a sampling of ten minutes will be sufficient to search for transits in the fainter sample of 400,000 stars, and for asteroseismology of hotter stars. For the small fraction of these faint stars for which a transit will have been detected, a 30 sec sampling will be applied.

2.8.11 Dynamical range

The planet search objectives of PLATO are based on the observation of stars as faint as $m_V = 13-14$, but stars as bright as $m_V = 6-7$ also need to be monitored for the detection of stellar reflected light on planet atmospheres and also for astrometric detection of planets.

Stars between $m_V = 6$ and $m_V = 11-12$ also need to be observed at a sufficient level for seismic analysis.

2.8.12 Summary of observational requirements

Table 2 gives a summary of the observational requirements discussed above. These can be translated into a first set of instrumental requirements, discussed in previous sections: collecting area $\geq 0.7 \text{ m}^2$; satellite pointing stability of the order of $0.2''$ on timescales of minutes; thermal stability of the order of 0.2 K/hr at detector and optics level.

2.9 The need to go to space

The science goals presented above require the detection of a large number of exoplanets and the detailed analysis of their central stars, including seismic analysis. They are achievable by a very high precision, very long duration and high duty cycle photometric monitoring from space of a very large sample of stars. The Earth's atmosphere provides strong disturbances which limit the achievable performance to millimag accuracies, mostly through scintillation noise. The small amplitude of the photometric dips caused by terrestrial planets are therefore beyond the range of ground-based observations. Scintillation noise in ground-based photometric observations also prevents the detection of low amplitude oscillations in cool stars. The noise in ground-based photometric observations is such that only giant planets with sizes larger than that of Saturn can be detected via their transits, while oscillations of cool stars are totally beyond reach of this technique.

In addition, long, uninterrupted observations, that only space-based instruments can provide, are neces-

sary to optimize the probability of transit detection, and to see several successive transits in order to measure the orbital period, as well as to avoid sidelobes in stellar oscillation power spectra.

Space is therefore necessary on one hand because of its tranquility and the absence of photometric disturbances, and on the other hand because of the possibility it offers to perform the long, uninterrupted observations that are needed to detect exoplanets and to perform seismic analysis of stars.

Alternative techniques can be used from the ground to achieve exoplanet detection as well as oscillation mode detection, and has seen tremendous progress in recent years. The most efficient of these relies on radial velocity measurements, performed in high resolution spectroscopy, with either echelle cross-dispersed spectrographs [7] or Fourier transform spectrographs [26]. In particular, the HARPS spectrograph installed on the ESO 3.6 m telescope at La Silla showed recently that it is capable of reaching radial velocity precision as low as about 1 m s^{-1} . Such a low level of radial velocity noise recently led to the discovery of a planet with a mass of $5/\sin i$ Earth masses on a close-in orbit around the $0.31 M_\odot$ M dwarf Gl 581 [42]. Although quite impressive, this performance cannot compare with those of a space photometric mission, and would not allow us to reach the science goals presented earlier.

One drawback of the radial velocity technique is that the mass determination suffers from the $\sin i$ ambiguity, except in the rare cases where the inclination angle i is known. For instance, the recently discovered planet around Gl 581 may well be a much more massive one whose orbit is seen at high inclination.

Second, there is a hard limit for the radial velocity precision achievable with this technique. A Doppler shift of 1 m s^{-1} corresponds to a spectrum displacement of about 10 nm on the detector of a HARPS-type spectrograph at $100,000$ spectral resolution. The data on which the recent exoplanet discovery around Gl 581 is based are not photon-noise limited, indicating that this hard limit has probably been met. Therefore, there is little hope for improving significantly the performance of the Doppler technique in the future. This means that smaller planets, with sizes and masses comparable to those of the Earth, will never be detected by this technique, and that the exploration of the exoplanet distribution down to at least Earth size, one of the most important science goals of PLATO, is not achievable from the ground.

Observations with HARPS have also revealed solar-like oscillations in nearby bright stars (*e.g.* [27]). However these observations have not allowed us to perform

sample	# of stars	mag. limit	field (sq. deg)	noise level (hr^{-1})	duration (years)	duty cycle	sampling (sec)	dynamical range
bright	100,000	11-12	≥ 300	8×10^{-5} goal 2.5×10^{-5}	3 (goal 4)	95%	30	$m_V=6-12$
faint	400,000	14		10^{-4}			600	$m_V=12-14$

Table 2: Summary of observational requirements

full asteroseismic analysis so far, for three reasons: *i*) the noise level is still too high to detect a large number of oscillation modes; *ii*) the day-night alternance creates strong day-aliases which pollute the power spectra and make their exploitation impossible; *iii*) the total duration of these observations is too short to allow us to measure the oscillation frequencies with a sufficient accuracy. Besides, asteroseismology with the radial velocity technique is limited to stars with projected rotation velocities smaller than about 10 km s^{-1} , which makes the list of accessible targets very limited.

There is little hope to improve significantly these three major drawbacks of ground-based asteroseismology. The noise level will not be easily decreased further, as discussed earlier. Moreover, these observations will remain severely limited in terms of target magnitude and $v \sin i$. Seismology programmes with HARPS are limited to stars with $m_V \approx 6$, above which photon noise is simply too high to allow us to detect any oscillation mode. In order to reach stars with $m_V \approx 11$, which is needed to study open cluster members for instance, much larger telescopes with diameters of the order of 40m should be used. High efficiency, high stability, high resolution spectrographs for these extremely large telescopes will be difficult to build, and obtaining high duty cycles for long periods of time on these telescopes is out of question, as detailed below.

The duty cycle of ground-based observations can be improved by multi-site networks of telescopes equipped with appropriate spectrographs; however, even if such an ambitious ground-based network can be setup in the future, the drift of sidereal time limits to only a couple of months the total time during which a high duty cycle can be obtained. An attractive alternative is to perform these observations from Antarctica. However, even in the overly optimistic scenario where an extremely large telescope would be installed in a high quality site in Antarctica, such as Dome C, and made available exclusively to asteroseismology programmes, the total duration of high duty cycle observations would not exceed three months.

We therefore conclude that asteroseismology from the ground with the Doppler technique, which has al-

ready been achieved on a few targets with modest duty cycle and total monitoring time, will remain limited to bright stars with low projected rotation velocities, and high duty cycle observations will be very rarely obtained and for limited total amounts of time.

3 Mission profile

3.1 Orbit

One of PLATO's top level requirements is the possibility of conducting very long observations in a stable environment, with as few interruption as possible. This requirement naturally rules out low-Earth orbits, for which there are strict limitations in terms of "continuous viewing zone" (see CoRoT or MOST mission scenarios). Also, low-Earth orbits suffer from high radiation levels (*e.g.* due to South-Atlantic Anomaly passes) as well as from very high scattered light contamination for the telescope from the sunlit Earth. Finally, ground-station contacts are short. These three issues are well-known major limitations of the CoRoT satellite, located on such a low-Earth orbit. Geostationary orbits or highly eccentric orbits with a high perigee, have better characteristics, but are very costly, and may still suffer from high levels of scattered light contamination as well as from eclipse seasons. We are led to propose a large Lissajous orbit around the L2 point. A large Lissajous features a limited cost of transfer from the Earth and is not affected by too many Earth-Sun or Moon-Sun eclipses. Besides, in the specific case of a reasonable satellite-to-ground telemetry rate (200 kb/s) as proposed for PLATO, one can easily manage the antenna lobe geometry with respect to the half-year parallax on the radio frequency line of sight (steering function). A preliminary ΔV budget will be similar to that of the *Herschel* observatory mission, with about 50 m/s for removal of launcher dispersion, 15 m/s for perigee velocity correction and 15 m/s for orbit maintenance. With margins, the PLATO SVM can be designed with a capacity of 100 m/s. Another advantage of a L2 orbit is to reduce dramatically the sources of noise related to the interaction between the

spacecraft and its environment.

Radiation impacts at L2 will affect in a limited way the photometric performances of PLATO. This problem is well known for missions in low-earth orbits, such as CoRoT, which suffer repeated passages in the South Atlantic Anomaly, but still succeed in providing ultra-high precision photometry. The radiation environment on a large Lissajous orbit around L2 will be less hostile, and dominated by solar eruptions. Since the first Cosmic Vision M-class mission will be flown around solar minimum, the effect of radiation impacts should remain limited, and in any case much lower than that of CoRoT. We also expect a lower impact of radiations on the mission performances than *e.g.* for *Gaia*, because PLATO will work at much higher photo-electron flux, thus minimizing the effect of electron traps produced by radiation impacts.

3.2 Launcher

The current assumption is to launch PLATO with a Soyuz/Fregat from Kourou. This launcher, available at a reasonable price, is extremely reliable, and its performance is well matched to PLATO's requirements. The mission strategy foresees that the Soyuz rocket will inject the PLATO/Fregat assembly in a low ($\simeq 200$ km) parking orbit, from which a firing of the Fregat upper stage will inject the PLATO spacecraft into an escape track toward the final L2 orbit.

3.3 Ground station visibility

The geocentric distance for the selected orbit (which closely approximates the range to any terrestrial ground station), varies between 1.2 million km and 1.75 million km throughout the operational lifetime. Any ground station located reasonably close to the equator will see the spacecraft as a quasi-stationary point, similar to a celestial body, for almost 12 hours per day. As the velocity of the spacecraft is nearly negligible, the observed range-rate effects will be induced almost exclusively by the Earth rotation.

35-m ground stations belonging to the ESA network, such as Cebreros (Northern Hemisphere) or New Norcia (Southern Hemisphere), can be used for spacecraft operations and scientific telemetry reception. Contrary to other space missions at L2, PLATO is compatible with communications in X-band.

3.4 Mission lifetime

The search for planetary transits necessitates a total duration of the observations of at least three years,

preferably four, in order to allow for definite detection of planets with orbital periods above one year. An additional phase of about one year must be added, in order to perform a series of shorter duration observations, as detailed in Section 4.1.1. The mission lifetime must therefore be at least four years, preferably five.

The transfer time toward the Lissajous orbit is typically 90 ± 20 days, depending on the day of launch along the year.

3.5 Science operations

The ground segment of PLATO may be built in similarity with that planned for *Eddington*, and be composed of three distinct elements:

- A Science Operations Center (SOC), with the responsibility of scheduling and preparing the observations, as well as performing the routine analysis of the data.
- A Mission Operations Center (MOC), converting the schedule and the instrument configuration commands into spacecraft commands, and receiving the telemetry stream back from the spacecraft.
- A PI-funded Science Data Center (SDC), which will be responsible for the pipeline processing of the data, leading the final mission products, *i.e.* the calibrated stellar light curves. It is also responsible for the set-up and running of the PLATO data archive, through which the data will be made available to the community. A copy of the archive will also be made available through the SOC.

Many components of the MOC and SDC pipelines will inherit from CoRoT experience.

4 Instrumental concepts

We have consulted European space industries in view of obtaining an independent assessment of the proposed concept. Thales-Alenia-Space and Astrium Satellites agreed to perform preliminary, self-funded studies. The concept principles were provided by the science team, without specific design constraints for allowing the widest possible exploration of solutions. Two different concepts, involving different observational strategies, have been proposed and investigated.

4.1 The “staring” concept

4.1.1 Observation strategy

In the staring concept, a first phase of the mission, with a duration of typically three or four years, is spent observing continuously the same field. This field is

chosen to provide a sufficient density of stars to comply with the requirements in terms of stellar sample (Section 2.8.2), as well as to contain stars presenting a specific interest for the seismology objectives of the mission, *e.g.* open clusters. A first, very preliminary examination of stellar catalogues indicated a field near ecliptic coordinates (210° , -60°) as a good potential choice. This field is near the galactic plane, has a high density of stars, and contains a large selection of open clusters offering a complete age sequence.

During this first staring phase, the field is observed continuously with a duty cycle close to 100%. The satellite is rotated around the line of sight by 30° every month, in order to keep a correct orientation of the solar panels and of the payload with respect to the Sun. The focal plane accommodation is such that stars are permanently on the detector mosaic, in spite of this satellite rotation. The station acquisition phase associated to each rotation, built on the model of what is done for CoRoT, will last less than one day (same field, stable environment making calibrations easier).

This staring phase will be followed by a “step and stare” phase of typically one additional year, where the payload will be pointed successively to several additional fields, each one monitored continuously for one to several months. The goal of this second phase will be: *i*) to extend to other regions of the galaxy the exoplanet statistics for planets on orbits shorter than a couple of months; and *ii*) to optimize the sample of stars of the seismology programme.

One very attractive possibility would be to use this phase for the systematic observation of potential targets of future space interferometric mission. This would allow us to measure precisely the characteristics of these stars, including a measurement of their age with a typical precision of the order of 10 – 50 Myr. The targets for space interferometry could therefore be sorted by age, allowing an optimization of the programmes on planetary atmosphere evolution with time.

4.1.2 Proposed payload

The science objectives of PLATO require both a very wide field of view ($\geq 300 \text{ deg}^2$) and a large collecting area ($\geq 0.7 \text{ m}^2$). The very wide field of view requires a short focal length yielding a large plate factor, which implies the use of a small pupil, since the optics cannot easily be made faster than $f/1.5 - f/1.3$. In order to comply with the collecting area requirement, we propose to use a large number of identical small size optics, each one coupled to its own focal plane, all of

them observing the same stellar field.

The concept of a large number of small pupil optics has at least three main advantages. First it complies with the stringent requirements in terms of signal-to-noise and field size. Second it provides a very high level of redundancy: if one or even several of the cameras fail, the photometric performance will not be severely affected; a loss of 10% of the cameras, in the very worst case, will result only in a 5% decrease of the SNR; we can also take advantage of this high level of redundancy for somewhat relaxing the specifications of the detector characteristics, thus severely reducing the costs. Finally, the large number of pupils offers the advantage of reducing the pointing stability requirement, by distributing on many pixels the flux of a given star; by averaging the many individual light curves, the system will behave as one single detector with an ultra-homogeneous pixel-to-pixel response.

Figure 8 shows the proposed payload on the recurrent *Herschel* platform, which is foreseen for this mission.

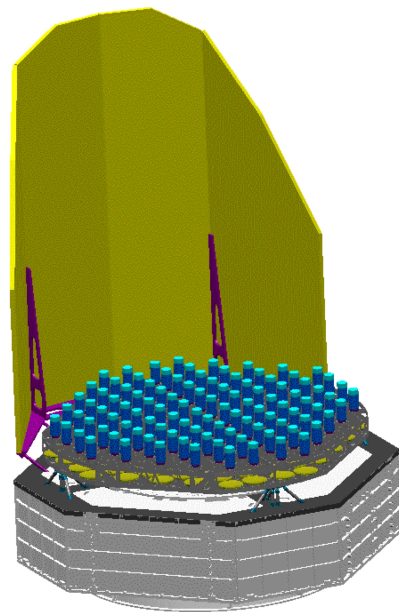


Figure 8: view of the payload integrated on full recurrent *Herschel* SVM.

The majority of these small pupil optics will be devoted to the study of faint ($m_V \geq 9$) stars in the field, using an elementary exposure time minimizing the losses during camera readout. For the observation of brighter stars that saturate the detectors with this exposure time, the plan is to use a small number of telescopes, with shorter elementary exposure times.

In addition, three of the telescopes can be used to ob-

serve the field in three different broadband filters (*e.g.* Johnson UBV). This would provide, at a very small cost in terms of photon loss, a full and homogeneous colour analysis of all stars in the field. These colours, completed by parallaxes of the same stars measured by *Gaia*, will allow us to place very accurately the observed stars in the HR diagramme.

Optical design

Description: the concept (Figure 9) consists of 100 identical axi-symmetric compact cameras, each one covering the same annular field of view between 13° and 6° radius. The optical design is based on a One Mirror Anastigmat (OMA) already proposed for the *Eddington* mission. Its advantage is its capability to work with fast aperture and wide field of view. A second advantage is that the 100mm pupil is placed on the first lens of the corrector so that the total mass is minimised by decreasing the lens dimension. On the other hand, the mirror diameter (240 mm) is larger than the pupil size, due to the pupil scan generated by the field of view (26°). With a focal length of 227 mm, the plate scale is $1.1 \mu\text{m}$ per arcsec. The optical performance is optimised to get a homogeneous spot inside this field, when a defocus of $-50\mu\text{m}$ is applied. The spot size in this case varies between 25 and $35\mu\text{m}$, *i.e.* about two to three pixels, across the field.

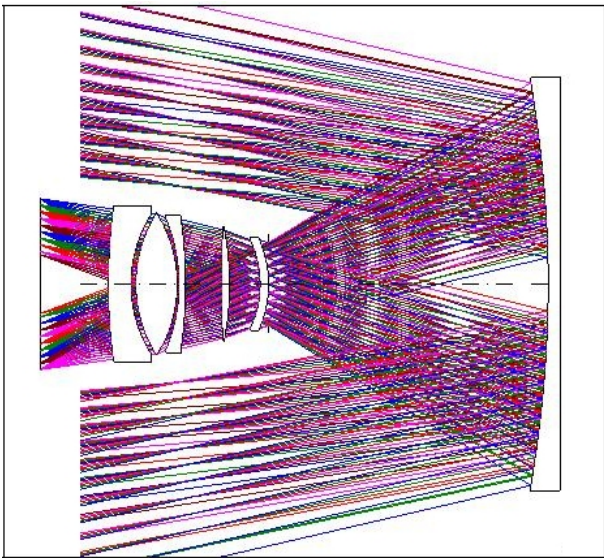


Figure 9: Optical design of the individual cameras. The prime mirror has a diameter of 240mm.

Optical performance: the goal is to have a PSF FWHM maximum increase of 20% at end-of-life (EOL). This implies reasonable tolerances: more specifically, the alignment tolerance between the mirror and the lens is about $5\mu\text{m}$ on each axis, compatible with 3D alignment measurement accuracy. The proposed breakdown in

PSF degradation at EOL is shown below:

manufacturing & characterization		7%
on-ground alignment	mirror	3%
	lens	3%
	detector	1%
	TOTAL	4%
ground-to-orbit	launch & hygro	0%
	ground-to-orbit thermoelastic	2%
	in orbit thermoelastic	0%
	TOTAL	2%
margin		5%
TOTAL PSF FWHM increase		$\leq 20\%$

The design is optimized for vignetting, so that the obstruction is minimum in the annular FOV. The highest obstruction is 45% at 6° and the lowest one is 12% at angles $\geq 10^\circ$ (Figure 10).

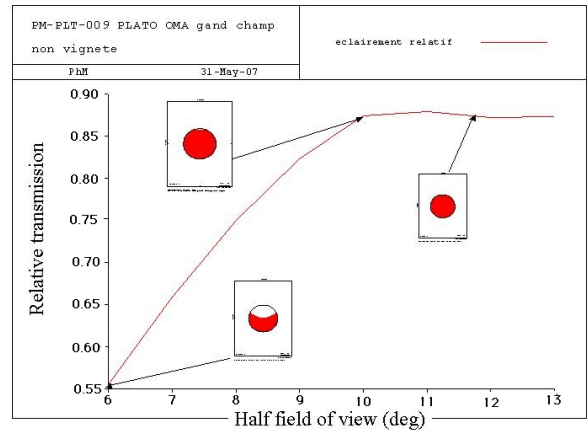


Figure 10: Variation of obstruction in the field.

Straylight: the design is robust to contamination, so that no specific cover is needed. With 5000 ppm on M1, the Point Source Transmission (PST) of this optical design is around 10^{-11} per pixel, which we have verified is acceptable. Two main straylight contributions have been identified and quantified:

- light from bright stars can be scattered by 5000 ppm of dust on the mirror, and fall on the focal plane. Intrinsic variations of these bright stars will perturb the photometric monitoring. As a very worst case, scattered light from $m_V=0$ star with a 0.1% photometric variation would produce a straylight modulation equivalent to $m_V=25$, well below the photon noise of the sources to be observed.

- out of field sources can be scattered into the field of view by the mechanical structure. These sources include for instances planets of the solar system. They can be discriminated *a posteriori* because they will not be imaged in the same way by all the cameras.

Dispersive system (optional): the coloured informa-

tion required by some of the science objectives (Section 2.8.9) can be obtained by introducing a dispersive system in the optical design, for instance a small angle prism. Although its dispersion is higher in the blue than in the red, which is not favourable for the scientific performance, the development of a prism seems less risky than that of low dispersion gratings. This trade-off shall be analysed further in the assessment phase. The introduction of a prism in the optical beam, completed by the construction of appropriate numerical masks for the aperture photometry algorithm, will result in the production of light curves in three colours, in a similar way as in CoRoT.

Mechanical architecture

The payload is made of 100 identical collecting mirrors, each one focusing through barrel lenses to a CCD focal plane (Figure 11). Mirrors are foreseen to be manufactured in last Cescic version HbCescic allowing mirror area density of 13 kg/m^2 (performance today under validation in the frame of ULT ESA project).

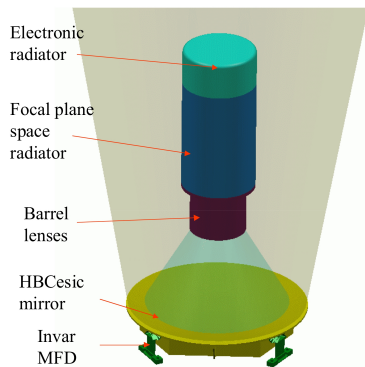


Figure 11: View of individual camera.

In order to be cost and mass effective, as well as to ensure a good mechanical stability, and a large amount of modularity, facilitating development, manufacturing and integration, the cameras can be mounted by groups of 25 in a single monolithic structure (Figure 12), whose design takes advantage of the technological and manufacturing capabilities offered by the today mastered Thales/ECM Cescic ceramic technology.

The Cescic monolithic structure is made of integrated upper and lower panels. The lower panel is made of a skin with ribs, while the upper panel is made of a rib pattern mesh, both linked together by integrated ribs outside the field of view of the instrument. The rib pattern holds all the objectives with the focal planes and the harness; the lower panel holds the mirrors. Such of design is easily manufacturable in one piece in

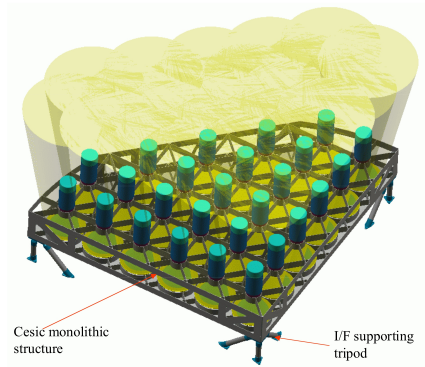


Figure 12: View of 25 cameras inside a single monolithic integrated Cescic structure, with lateral size of 1590mm.

Cescic, ensuring very high stiffness and stability.

The assembly and alignment of the 25 cameras in the Cescic structure will be cost effective thanks to the Cescic capability to perform, by EDM, very precise I/F. After independent characterisation, the mirrors will be finely screwed through MFD directly to the Cescic structure. The exact position of the lens barrels and focal planes will be determined by fine 3D measurements, aligned through micro control tables and then screwed (or glued) on the Cescic structure.

After independent tests, the four quarters are integrated through three-point isostatic bipods on a sandwich CFRP I/F payload baseplate (Figure 13).

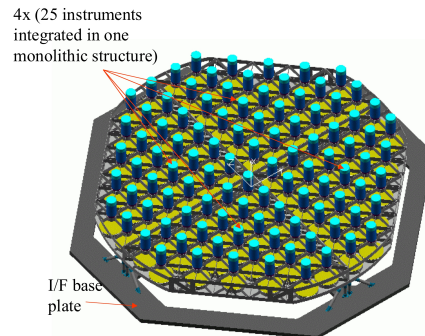


Figure 13: View of the 4 time 25 cameras (fixed on I/F payload baseplate).

Thermal concept

Overall thermal description: from a thermal point of view the PLATO spacecraft is a set of three sub-assemblies: the Sunshield/Sunshade (SS), the Instrument Assembly (IA) and the SVM. The main driver of the IA thermal design is the thermal stability needed to meet the pointing stability requirement. The main driver of the SVM thermal design is to minimize the

modification from *Herschel* in order to keep the highest recurrence possible. Such constraints lead us *i*) to implement an SS screening the incident solar flux on the whole IA, a part of which is also used as a Solar Array; *ii*) to decouple IA from SVM to avoid that the SVM thermal instabilities are passed to the IA.

SVM thermal concept: the differences between PLATO and *Herschel* impacting the thermal design are:

- different satellite attitude, due to different pointing strategies
- different accommodation of PLM warm units in the SVM.

Although the electrical unit accommodation is not yet defined precisely for PLATO, it will be possible to optimize it easily inside the SVM as already designed for *Eddington*. Each equipment will be maintained in a common temperature range of $[-10 - +50^\circ \text{C}]$.

Instrument thermal concept: the PLM sides are protected from Sunshield and SVM indirect radiative effects by MLL. The focal plane is passively maintained at -100°C . The temperature of the primary structure and optics of each telescope can be regulated either at 20°C or at -100°C . The worst case from a thermal point of view is to have the instrument regulated at ambient. A simplified model built with Thermal Control Design Tool (developed under ESA TRP) allows to check the possibility to control each camera at 20°C and to perform a pre-sizing of radiators to maintain the focal plane at -100°C and electronics around 0°C . The resulting needed total power in this case is around 200 W (including 25% margin), which is compatible with *Herschel* SVM capability.

A full thermal study was performed for *Eddington* to estimate the SS and SVM impacts on the telescope and FPA thermal stability. With a very similar mission definition and architecture, PLATO instrument temperature stability will comply with the requirements.

Focal plane concept

Focal plane architecture: the focal plane consists of four panels, each of them containing 25 identical cameras.

Each focal plane is made of several identical detectors. A preliminary analysis led us to the choice of detectors with square pixels of $13 \mu\text{m}$, a well-proven technology. Many possibilities can be proposed for the actual size of the chips and their accommodation. Two of them are given in Figure 14, based on $2\text{K} \times 3\text{K}$, or on 800×1800 pixel CCDs.

The CCDs are defocused to produce a PSF varying across the field between 2 and 2.5 pixels, *i.e.* between 20 and $30''$. This defocusing is needed both to avoid saturation while collecting large photon fluxes, and to limit the impact of satellite jitter on the photomet-

ric performance. We have checked that, with this size of PSF, and with the preliminary choice of field presented in Section 2.8.3, the level of contamination of programme stars by background stars down to $m_V = 17$ will remain acceptable. Note also that the size of the PSF in the exoplanet channel of CoRoT is very similar ($30''$), and yet the contamination of the faintest CoRoT programme stars, which are fainter than those of PLATO ($m_V = 15.5$ instead of 14), is acceptable [3].

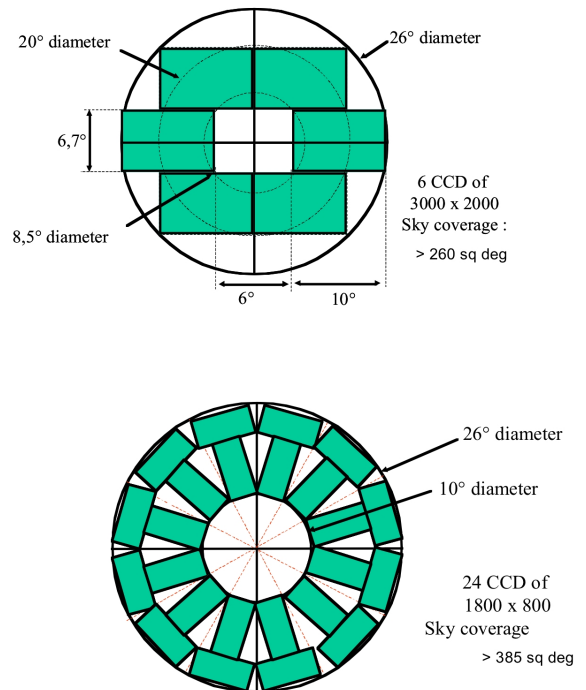


Figure 14: Two possible accommodations for populating the focal plane.

Very bright stars saturating a fraction of a CCD will not affect the other detectors of the same focal plane.

Ninety telescopes will be dedicated to the observation of stars fainter than $m_V = 9$, while ten telescopes will be used for the observation of brighter stars. The individual integration time for stars fainter than $m_V = 9$ is 32 s. An output frequency of 2 MHz/CCD will be used in order to read out each chip in less than 3 s in case of $2\text{K} \times 3\text{K}$ matrix, and in less than 0.7 s for 800×1800 matrix, hence the on-sky efficiency will be better than 90% in all cases. The full-well capacity of the CCD pixels is 250,000 electrons.

The detectors devoted to bright stars, which will be windowed, will have a shorter integration times, typically of 1 s. Their readout will be synchronised with that of the other focal planes, in order to use the same

electronics for all CCDs.

Electronic modules: highly integrated electronics module will be used in order to minimize the volume allocated to the focal plane.

Each Proximity Electronics Module is constituted of a CDS circuit, an ADC, circuits of clock generation/distribution for CDS/ADC/CCD and interfaces with the data-handling subsystem. Power supplies and Master Clocks will be located further from the focal plane and will manage several electronics modules.

The dissipated power is expected around 2.4 kW for the overall electronics system. The dissipated power due to the CCDs themselves will be around 300 W in total. The overall dissipated power at instrument level (100 cameras) is near 2.7 kW which is compatible with the proposed thermal concept.

Onboard data processing & downlink rates

Although the payload electrical architecture is still open and subject to trade-off, one can functionally divide the onboard treatments into five functions for each camera (for $m_V \geq 9$), as shown below:

function	# of stars	lightcurve sampling	coding (bits)	volume (kbits/s)
aperture photometry, primary stellar sample				
F1	100,000	32 sec	16	150 (1)
aperture photometry, second stellar sample				
F2	400,000	600 sec	22	46 (1)
line of sight calibration, star centroid $\Delta x, \Delta y$				
F3	50	32 sec	16	0.3
astrometry, star centroid $\Delta x, \Delta y$, primary stellar sample				
F4	100,000	600 sec	16	5.6
background photometry, dark signal				
F5	a few hundred	32 sec	16	0.1

(1) The camera telemetry volumes for F1 and F2 are divided by 3 if the option of producing 3-colour light curves through a dispersive device is not implemented.

Taking into account the inertial pointing of the instrument with stars assigned to keep a constant position on the CCD, the aperture photometry can be performed with fixed photometric masks. To process the huge amount of collected data, it is foreseen to apply the windowing and the individual light-curve and centroid processing as close as possible to each focal plane. With some elementary computing power at immediate proximity of each camera, the amount of data can therefore be reduced from 18 Mbits/s to roughly 200 kbits/s. This elementary computing function is likely to be performed by local ASIC.

On the ten cameras dedicated to bright stars (m_V between 6 and 9), the number of targets will be small and windowing can be applied at CCD level.

Downstream from the complete set of cameras, one or several central processing units (calculators) will multiplex, compare and average the 100 lightcurves for each star, and compress the photometric data. The

central processing unit is also in charge of computing the average centroid measurements both for line of sight calibration (jitter correction on light curves) and delivery of payload depointing angles to the SVM AOCS, in a similar way as what has been done on CoRoT or studied for *Eddington*. Before compression, the mission data rate is estimated at 340 kbits/s. By implementing a DPCM loss-less compression algorithm, expected to be particularly efficient and reliable on photometric time series (small signal variations close to a stable mean value, no scientific correlation between targets), the global data rate between the payload and the SVM is assumed to be close to 140 kbits/s (compression factor around 2.5). This is fully in line with the current SVM capabilities.

Concerning payload internal communications, trade-off between SpaceWire and point-to-point links remains to be done. The SpaceWire technology is well adapted to the large number of inputs/outputs, makes it possible to concentrate the data and can be used up and down (including command and control of the proximity electronics modules). The final choice should take into account the desired level of versatility.

There is no calibration device installed on board, and calibrations needs (sky recognition, geometric and radiometric characterizations...) should be met without applying additional constraints on rates or storage capacities. Full frame images are downloaded during specific calibration phases.

4.1.3 Expected performance

The performance of the design presented above was first estimated in terms of number of accessible targets and achievable level of noise. We have used the preliminary analysis of the stellar content of test fields, presented in Section 2.8.3 and Table 1.

Because the field obstruction varies significantly across the field, targets with the same magnitude are not observed with the same level of noise across the field. In other words, a given level of noise will corresponds to stars with different magnitudes at different locations in the field. We have chosen to display the expected performance in terms of number of targets observable with various levels of noise. These predictions, which are summarized in Table 3 are compliant with the basic requirements of this mission, since we can observe more than 100,000 stars at a noise level better than 2.6×10^{-5} per hour, and up to 360,000 stars with a noise better than 8×10^{-5} per hour.

The proposed design can also achieve a very high photometric and astrometric precision for the observa-

noise		#		mag
ppm/hr	ppm/30 d	stars	dwarfs	range
10	0.4	10,000	5,200	9.3-9.9
15	0.5	21,000	11,000	10.1-10.7
20	0.7	49,000	25,000	10.7-11.3
26	1.0	101,000	52,000	11.3-11.9
53	2.0	263,000	137,000	12.8-13.4
81	3.0	360,000	187,000	13.7-14.3
100	3.7	410,000	213,000	14.2-14.7

Table 3: Number of stars observable with various levels of photometric noise.

m_V	# stars	noise ppm/hr	noise ppm/30 d	astrom. noise/30 d (μ as)
6	85	6.4	0.3	6
7	270	11	0.5	10
8	810	17	0.8	15

Table 4: Bright stars observable with PLATO.

tion of very bright stars in the field. Table 4 summarizes the performance. The calculations assume that stars brighter than $m_V=9$ are monitored with ten telescope units only. The astrometric precision is computed assuming that the measurements are limited by photon noise and that the centroid of each star is measured with reference to those of all other stars in the field. The number of stars given are only order of magnitude indications, since they will depend on the exact position of the field, as well as of the orientation of the CCD pattern in the field. The performance summarized in this Table show that giant exoplanets on close-in orbits can be detected around bright stars, using the photometric modulation due to scattered stellar light on the planet atmospheres, while the astrometric wobble of the stars produced by exoplanets with Jupiter mass orbiting their stars at typically one AU are detectable at least down to $m_V=8$.

4.1.4 Basic spacecraft characteristics

Satellite architecture

The payload is easily accommodated on existing fully recurrent *Herschel* SVM (Figure 8). The payload is protected from the Sun with a large sunshield allowing to observe stars up to 45° from the Sun giving therefore the opportunities to cover large angular fields. The sunshield holds the solar cells and its design is close to that of *Herschel*. The solar cell area will be scaled

down for PLATO power needs.

A preliminary mass budget is given below, with a total mass of 1997 kg including margin at subsystem level and a 20% system margin, showing a clear compliance with Soyuz launch capability from Kourou to L2 transfer orbit.

Items	material	unitary mass		total mass		margin %	max mass Kg
		Kg	number	Kg			
Sunshield				53			64
panels	cfrp sandwich		14,00	2	28,0	20,0	33,6
fixation system (beam +inserts)	al+ta6v.		13,4	1	13,4	20,0	16,1
CTP(mil+paint)+solarcells			12	1	12,0	20,0	14,4
payload I/F baseplate				36			43
I/F payload panel	cfrp sandwich		20,67	1	20,7	20,0	24,8
inserts	ta6v		0,03	150	4,5	20,0	5,4
ctactp +cabling			11	1	11,0	20,0	13,2
INSTRUMENTS				638			768
equipped mirror M1	Hbcesic+hrvar		0,65	100	65,0	20,0	78,0
monolithic structure	cesic+insert		33,00	4	132,0	20,0	158,4
lenses+barrels			1,3	100	130,0	20,0	156,0
CTP CTA	CTP CTA		0,50	100	50,0	20,0	60,0
electronics +PF	elec		2,20	100	220,0	20,0	264,0
cabling	elec		0,25	100	25,0	20,0	30,0
supporting beams	cfrp+ta6v		1,35	12	16,2	20,0	19,4
Electronics					55		66
Video	elec				30,0	20,0	36,0
PDHE	elec				15,0	20,0	18,0
alarm payload	elec				10,0	20,0	12,0
TOTAL PAYLOAD					783		939
SL : SVM Herschel					615	0	615
ERGOL L2					100	10	110
TOTAL					1498		1664
system margin						20	333
TOTAL WITH MARGIN							1997

Spacecraft assembly compatibility with Soyuz fairing has been also verified (Figure 15) and an important margin exist allowing future potential design evolution of the payload and sunshield .

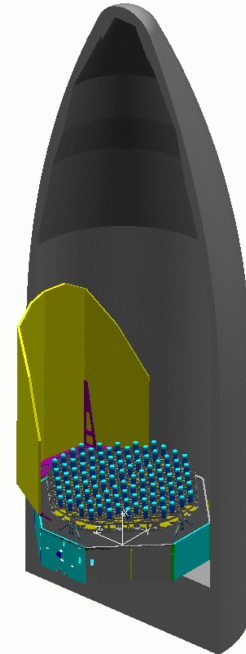


Figure 15: Spacecraft assembly under Soyuz fairing showing volume compatibility.

Moreover, the concept based on 100 identical telescopes can be easily adapted by adding telescopes to increase the final scientific performance or by remov-

ing some of them in order to comply with the mass and/or the cost requirements. The best compromise between performance and system constraints (mass, cost, power) can be easily reached with such concept.

Service module

The *Herschel* SVM has been selected as service module for PLATO satellite. The *Herschel* SVM, although designed for a shared Ariane V launch, fits inside the Soyuz ST fairing without major modifications. A new inverted cone adaptor needs to be designed for the Soyuz launcher to cope with the bottom diameter of the primary structure of the SVM.

The payload mass (940 kg) is fully compatible with the supporting load capability of the *Herschel* PF, leading to the reuse and benefit of the *Herschel* qualification SVM.

The mission delta-V has been computed to 100 m/s for a similar Lissajous orbit as *Herschel*. This requires only 100 kg of propellant (far less than for *Herschel*), leading to a smaller propellant tank.

The two current 1553 protocol data buses (with effective capacity of 350 kbps allocated to the PL) designed for telemetry and telecommand data onboard are sufficient for PLATO needs.

The current mass memory is designed to store onboard about 24 Gbits of data. Considering the PLATO data rates between 12 and 15.5 Gbits/day, this mass memory is saturated in two days of continuous operation without download of data to ground, which is considered acceptable.

The satellite attitude is derived with a maximum precision of 2.4". The precision of the system can be dramatically improved to better than 0.2" by the introduction of a pick-up mode integrating the payload signal (coming from the camera dedicated to bright stars) into the AOCS system. This solution has been successfully implemented on the CoRoT satellite, and has been studied in detail for *Eddington* which was planning to use the *Herschel* platform as well.

Downlink rates

The current data rate between the *Herschel* SVM and the Earth is 1.5 Mbits/s (during the three-hour daily communication periods). Since the storage of 2 days of data is possible for PLATO, the current downlink capabilities of the *Herschel* SVM is considered compliant with the PLATO mission.

However, the *Herschel* transponder is no more in production and will be substituted for future missions by the DST (Deep Space Transponder) in development at Thales Alenia Space Italy for *Bepi-Colombo* and other missions (see Section 4.1.5).

4.1.5 Technological readiness

Most technologies proposed for PLATO are flight proven (TRL 9). The only technologies involved which have lower levels of maturity are described below.

At payload level

Lightweight HbCesic mirror technology is a key issue to limit telescope mass, such technology is today under development and qualification through ESA ULT project. A mirror of 600 mm with 10 kg/m² is now under manufacturing after full design and analysis optimisation. Polishing performances of such lightweight mirror have been already evaluated and are fully in line with PLATO optical requirement without having to request costly ion beam or CPM polishing techniques.

One other key issue for the mass of the instrument is the use of lightweight monolithic Cesic bench holding both mirrors and focal planes. Such type of bench has been already manufactured, qualified and tested down 30 k showing its very high stability and strength.

At the time of the phase B of PLATO, all these technologies will be TRL 9 thanks to programmes in progress at Thales Alenia Space (*e.g.* Spirale, to be launched in 2008).

At SVM level

The TTC is composed of a couple of LGA antennas, a MGA antenna, two X-band transponders with two TWTA and one RFDN. The TTC subsystem is the most critical one due the unavailability of recurring transponder. The *Herschel* X-band transponder is indeed no more produced. A new development is foreseen for *Bepi-Colombo* and *ExoMars* missions (TRL8).

4.1.6 Programmatics and costs

The concept using 100 identical cameras is based on very mature technologies. The main originality of the proposed solution will be in its alignment and verification philosophy.

Alignment and test philosophy:

Thanks to the tolerant optical solution in terms of misalignment (small camera) and thanks to the huge number of cameras, a new alignment and verification philosophy can be proposed (Figure 16). The idea is to align each camera (mirror vs lenses) by using a tri-dimensional machine (whose typical accuracy is compliant with the needed tolerances), making the alignment of the 100 cameras easy, fast and cheap.

A new statistical approach for the verification phase can also be proposed. The final performance (encircled energy) can be measured only on a limited number of cameras (*e.g.* 10 to 20) in order to derive the statistical characteristics of the whole instrument. If in the end,

up to 10% of the cameras are out of compliance or lost, the impact on the final performance remains very low: the decrease in SNR is only about 5%, which is still acceptable for the mission.

Such statistical approach is also foreseen to be applied for the CCD procurement: if some pixels, rows or columns are not usable, it is not a real problem since statistically, it is quite impossible to have all bad pixels for each camera located on the same sky area. The final manufacturing rejection and the acceptance tests can be largely relaxed inducing a large cost benefit.

Model philosophy

The development philosophy is to validate very early the alignment based on the Tri-dim machine use. A breadboard constituted by a representative mirror and lenses, developed during phase A, can be used to realise several alignments (more than ten) in order to statistically demonstrate the compliance of this method and to measure its dispersion.

Thanks to this demonstration, it will be possible to propose directly a proto-flight model of the instrument. In case of problem, it will be easy in this concept to replace a broken camera by a spare one. It can even be decided to use the instrument as is, as long as the number of dead cameras remains lower than 10%.

Costs

The cost estimate of PLATO in the staring concept is based upon the following assumptions :

- the SVM is recurrent from *Herschel* with minor adaptations (LV interface) and takes benefit from *Herschel/Planck* hardware spares
- the heritage from HP and the experience coming from CoRoT should reduce the development cost of the ground segment and operations in a routine scenario (MOC and SOC)
- despite the large number of detectors, the robustness and the versatility of the design allows to limit the laboratory activities for chips characterization at a reasonable level and to accept partially faulty units.

The process of building and assembling a hundred "mass-produced" small telescopes shall lead to define a specific cost/risk trade-off management during phase 0 studies.

The reference industrial organization is assumed to be with one prime contractor in charge of delivering the integrated space segment and one prime contractor in charge of delivering the ground segment.

The focal plane assemblies (FPA), the on-board application software and the ground segment data processing algorithms are assumed to be delivered by partner laboratories or subcontractors funded by cooperation and are thus removed from the total estimated

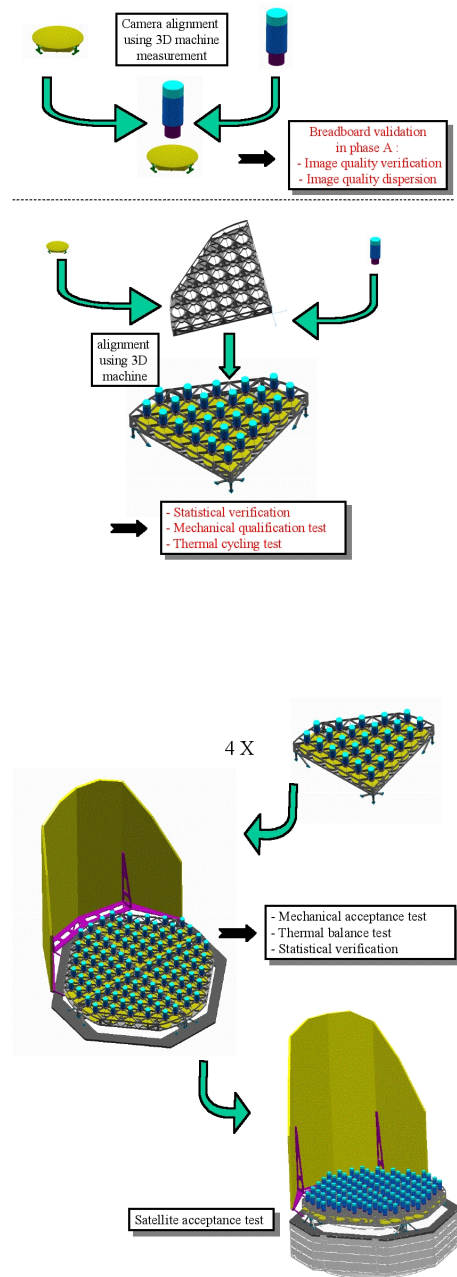


Figure 16: The integration and test philosophy.

cost for ESA.

All costs for spacecraft and payload (equipment, engineering, project office and AIT) were established by Thales Alenia Space on the basis of ESA equivalent programmes. The total estimated cost includes a 18% contingency margin, also covering design/cost uncertainties at system level at this step of the mission definition.

By default, some budget lines are fitted to the reference Main Cost Elements (MCE) given by ESA for

Class M Missions.

Activity	ROM (M€)	% of total (ESA part)	Comment
Pre-implementation (studies)	6	2%	ESA MCE
Spacecraft total estimated cost	217		
Spacecraft total industrial cost for ESA	148	51%	
SVM (product, project office, AIT)	92		
Payload (focal plane not included)	56		
Payload on-board software and processing units	9		Cooperation
Focal plane assembly (complete set)	60		Cooperation
Launch services from CSG (SF-2B)	40	14%	ESA MCE
Ground segment total estimated cost	24		
Ground segment total industrial cost for ESA	15	5%	
Calibration and scientific processing chains	9		Cooperation
ESA internal cost	30	10%	ESA MCE
Overall mission cost	317		
Contingency – provision for risks	42		
Design maturity margin (at mission level)	10	18%	ESA MCE
TOTAL estimated cost with margins	369		
TOTAL estimated cost with margins for ESA	290		

Estimated cost of PLATO in the "staring" concept

4.2 The “spinning” concept

4.2.1 Measurement principle

The spinning concept is based on the re-use of *Gaia* Service Module, and on the use of three telescopes of aperture 0.72 m^2 and FOV 23 degree^2 each. The concept enables terrestrial planet detection in solar-type systems for a sample of 144,000 stars by exploring a field of view larger than 1400 degree^2 , and the detection of planets with radii ≤ 4 earth radii in solar-type systems for more than 2,500,000 stars. Colour measurements can be included for enhancing transit discrimination. The instrument is operated in two modes: the search mode for planet finding and asteroseismology, and the fine observing mode for improving the planet transit measurements and for asteroseismology. The data rate is moderate in both modes.

The payload consists in a number n of identical telescopes observing in n directions regularly distributed on a great circle. When the entire system is rotated about an axis perpendicular to the great circle with a period T , each telescope will scan a band centred on the great circle of width equal to the telescope field of view (FOV) across scan (AC). Let $(\theta_{AL}, \theta_{AC})$ be the instantaneous telescope FOV along (AL) and across (AC) scan. Any object located in the scanned band will be regularly observed with a period T/n and an integration time per telescope $T \times \theta_{AL}/(2\pi)$. The design parameters $(n, \theta_{AL}, \theta_{AC}, T)$ and the collecting aperture are adjusted so as to enable the restitution of stellar oscillations in the range 0–10 mHz and to detect Earth-like planet transits at magnitude $m_V = 11$. Several sets of parameters can provide the same performance. The parameter selection constraints are: the allowable volume and mass, telescope accommodation, optics feasibility and minimum focal length for avoid-

ing star confusion.

A good compromise is obtained with $n = 3$ telescopes, of rectangular collecting aperture $0.9 \times 0.8 \text{ m}^2$, and a rotation period $T = 20 \text{ min}$. The use of Three Mirror Anastigmat optics provides a large FOV 5.9° (AL) $\times 3.9^\circ$ (AC) = 23 degree^2 per telescope. The design assumes a re-use of *Gaia* detectors, with a binning of 21 (AL) $\times 7$ (AC) pixels, providing a macro-pixel sky resolution of $12.4''$ with 3.5-m focal length, and a charge collection capacity of about $3 \times 10^7 \text{ e-}$ per macro pixel. The instrument parameters are summarised below.

Telescopes		
Number of telescopes	3	
Diamètre ALong scan (AL)	900	mm
Diamètre ACross scan (AC)	800	mm
Field AL	5.9	deg
Field AC	3.9	deg
Total FOV	23.1	deg
Focal length	3500	mm

Focal planes		
CCD detectors	Gaia AF re-use	
Pixel size (AL x AC)	10 x 30	$\mu\text{m} \times \mu\text{m}$
Number of pixels (AL x AC)	4500 x 1966	
Number of detectors AC	4	
Number of detectors AL	8	
Number of detectors per telescope	32	
Total number of detectors	96	
Operating temperature	~ 170	K
Pixel size on the sky (AL x AC)	0.59 x 1.77	arcsec
Pixel binning (AL x AC)	21 x 7	
Macropixel on the sky (AL x AC)	12.4 x 12.4	arcsec
Macropixel full well capacity	2.9E+07	e-

The system operating modes are detailed in below, assuming equal time sharing between the two modes.

For the search observing mode, the satellite is rotated so as to scan the galactic disk. This mode explores a FOV of about 1400 deg^2 for planet detection and enables potential terrestrial planet detection for more than 144,000 stars. It can also achieve asteroseismology of classical pulsators in the upper main sequence, such as *e.g.* $\delta \text{ Scu}$, $\gamma \text{ Dor}$, $\beta \text{ Cep}$, Be stars, whose pulsation frequencies are sufficiently low to be well sampled by the spinning procedure.

Search mode (Galactic disk scan)		
Rotation period	20	mn
Scan rate	0.30	deg/s
Explored field of view	1414	deg
Detector operation	TDI mode	
TDI step	0.55	ms
Integration time per detector	2.46	s
Integration time per telescope	19.6	s
Collected signal per hour, $V = 11$	1.5E+08	e-/h
1/SNR, per hour, $V = 11$	8.1E-05	
Number of observed stars, $V = 11$	144 000	stars
Number of observed stars, $V = 14$	2 500 000	stars
Data rate	130	kbits/s

For the fine observing mode, the instruments are

operated in staring mode for maximizing the observing time on selected areas that have been determined in the search mode. One of the telescopes is pointed to the galactic disk while the two others are exploring new areas of galactic latitudes below 60° . One can observe in fine mode up to one third of the stars that have been measured in search mode (plus extra stars due to the FOV extension and position).

Fine observing mode		
Field of view per telescope	23	deg
Total FOV	69	deg
Detector operation	Frame transfer mode	
Observation duration (typical)	30	days
Integration time (typical, $V = 11$)	30	s
Number of observed stars, $V = 11$	85 000	stars
Number of observed stars, $V = 14$	1 300 000	stars
Fraction of galactic disk covered	1/3	
Data rate	60	kbits/s

The data rates are comparable in both modes and remain moderate. The assumptions for the data rate evaluation are the following: (a) the three telescopes are treated independently; (b) the measurements are binned providing a single star signal per telescope transit (c) three colours are transmitted per star for $m_V \leq 11$ and (d) a conservative data compression rate of 2.5.

4.2.2 Observation strategy

The satellite orbit is about L2. In search mode, the spacecraft is simply rotated around the galactic pole axis to cover the galactic disk. Nevertheless, the Sun is rotating at year period in a plane inclined at 60° with respect to the galactic plane. The spacecraft is equipped with a circular sunshield as on *Gaia*, that protects the payload from direct solar illumination, up to a guard angle θ .

When the Sun is below the galactic plane, the spacecraft is rotated about the Galactic North pole direction, and when the sun is in North galactic hemisphere, the spacecraft is flipped upside down and rotated about the Galactic South pole direction (Figure 17). Between these two extreme positions, the spacecraft shall be orientated with its sunshield towards the Sun (within an angle of $\pm\theta$) to protect the payload from the Sun and one of the telescopes can be pointed towards a target in the galactic plane for the fine mode observation.

The observation strategy relies therefore on the separation of the year in two parts: one when the spacecraft is rotated to scan the galactic plane permanently and one when the spacecraft has a fixed three-axis control to point one of its telescope towards a selected target field. The partition of the year is a direct function of the sunshield protection angle θ and needs to be optimised with respect to science return. For the present

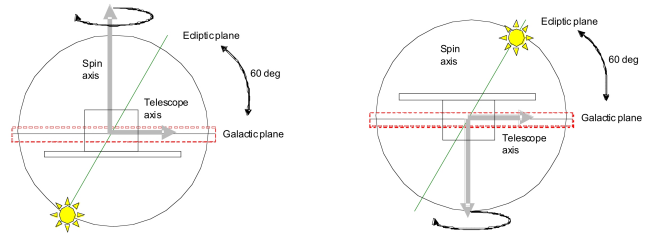


Figure 17: With a $\approx 40^\circ$ sunshield protection (re-use of *Gaia* SVM), the spacecraft scans the galactic plane during six months in the year and operates in fine observing mode during the other 6 months.

proposal, based on a re-use of *Gaia* SVM for best compromise between costs and performance, the angle θ is about 40° , and the spacecraft is naturally equally used in search and fine observing modes over a year.

4.2.3 Payload definition

The three telescopes are mounted on a common tore structure and use separate focal planes. The mirrors and the tore are made of silicon carbide, providing low mass and high stability. The telescope mirrors and the instrument structure are within current manufacturing capabilities.

The telescope optics is constituted of three aspheric mirrors (Figure 18). The pupil ($0.9 \times 0.8 \text{ m}^2$) has been located on the primary mirror and the inter-mirror distance was set about 2.2 m for accommodation purpose. The largest mirror is the tertiary M3 ($\approx 1.6 \times 1.2 \text{ m}^2$). Some further optimisations may reduce somehow the mirror size. It is important to note that the required spot diameter for PLATO is about $200 \mu\text{m}$ for the selected focal length 3.5 m. Therefore, the mirror optical quality requirements can be significantly relaxed, with a typical wavefront error accuracy of $\approx 2\lambda$. In comparison to *Gaia* or other similar diffraction limited telescopes, the mirror polishing specifications are relaxed by a factor ≈ 100 , which should reduce mass, development schedule, risks and costs. The mirror alignment requirements are also not critical and do not require a re-alignment mechanism in orbit. A very high telescope PSF stability will be obtained in orbit since the thermal stability of the assembly will be comparable to that achieved for *Gaia* ($\leq 50\mu\text{K}$). Such stability is not mandatory for PLATO and some mass savings related to thermal hardware could be envisaged.

Colour information can be obtained by locating a disperser close the focal plane. The use of a simple prism can be envisaged but it features non linear dis-

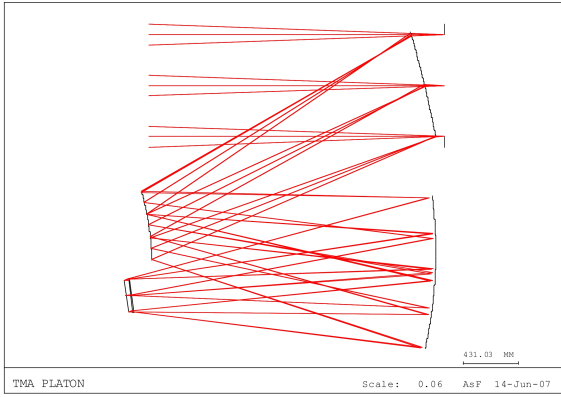


Figure 18: Optical design.

persion and degrades the spot diameter by a factor ≈ 2 . This should still be acceptable for the mission. The use of a low resolution grism provides much better performance: negligible spot diameter increase and quasi linear dispersion along scan. The spectrum length in the first order is then about $500 \mu\text{m}$, and the order confusion is achieved by limiting the wavelength range to $0.46 - 0.9 \mu\text{m}$ (typical). The grism achievable efficiency needs to be investigated, but the zero order provides anyhow useful signal that can be transmitted. The grism is part of the focal plane assembly and could be placed in front of each detector column if needed (Figure 19). Ghost images require specific investigations in future studies.

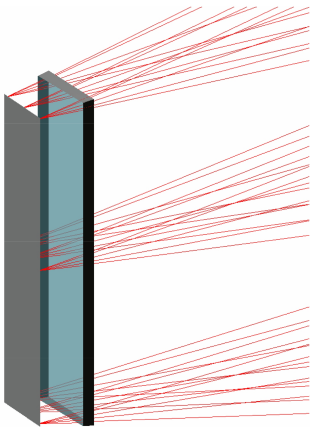


Figure 19: View of the grism disperser that is located in front of a CCD column. The disperser may be split in two parts across scan for easing its manufacturing.

The focal plane assemblies can be based on a strict re-use of the existing *Gaia* AF CCD. In fine observing mode, the transfer time is small in comparison to the integration time ($\leq 10\%$) and the observation can be

achieved without implementing a shutter, as already demonstrated in *Eddington* studies. As for *Gaia*, the focal planes are passively cooled at 170 K (TBC) for minimising radiation impacts. The *Gaia* AF CCD TDI gates can be used for reducing the integration time and managing the star magnitude dynamical range from $m_V = 4$ to 14, without detector saturation. TDI gates are also useful in staring mode for star position measurements at a high rate ($\approx 1 \text{ Hz}$) for AOCS purpose.

The overall payload mass is comparable to that of *Gaia*: the preliminary exercise indicates that the optics mass increase (estimation +120 kg, can be further reduced due to large optics tolerances) is merely compensated by the suppression or simplification of several *Gaia* equipments: RVS and related electronics, basic angle monitoring, M2 mechanisms, lighter video processing unit etc. The power and data rates needs are smaller than for *Gaia*. The mass of the PLATO payload is estimated near 650 kg, while its power consumption is around 650 W. The telescope and structure work temperature will be around 130 K. Figure 20 shows the payload assembly.

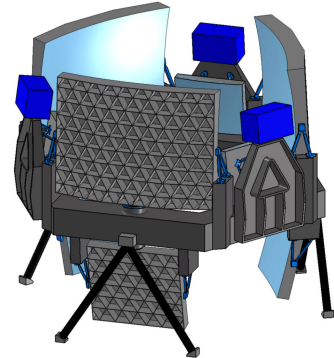


Figure 20: View of the payload assembly.

4.2.4 Expected performance

The overall performance of the “spinning” concept can be estimated in a straightforward way and are given in Table 5, in terms of expected number of stars observed at different noise levels both in search and fine modes.

As for the “staring” concept, we can achieve a very high photometric and astrometric precision for the observation of very bright stars. This approach will be particularly attractive in “search” mode when the whole galactic plane will be surveyed, and the use of programmable gates in the CCD TDI process will allow us to very bright stars without saturating the detec-

noise		#		mag
ppm/hr	ppm/30 d	stars	dwarfs	
search mode , duration 1825 days				
50		55,600	28,900	10
81		144,000	75,000	11
130		240,000	125,000	11.5
fine mode , duration 30 days				
20	0.7	85,000	44,000	11

Table 5: Number of stars observable with various levels of photometric noise.

m_V	# stars	noise ppm/hr	noise ppm/30 d	astrom. noise/30 d (μas)
6	290	9	0.4	8
7	930	15	0.7	14
8	2740	24	1.1	21

Table 6: Bright stars observable with PLATO in the spinning concept.

tors. Table 6 summarizes the expected performance.

4.2.5 Basic spacecraft characteristics

Spacecraft mechanical architecture

The spacecraft platform (Figure 21) is a direct reuse of *Gaia* service module (SVM), with the same structure, same Deployable Sunshield Assembly and with a similar thermal tent for the payload adjusted in geometry to PLATO need spacecraft.

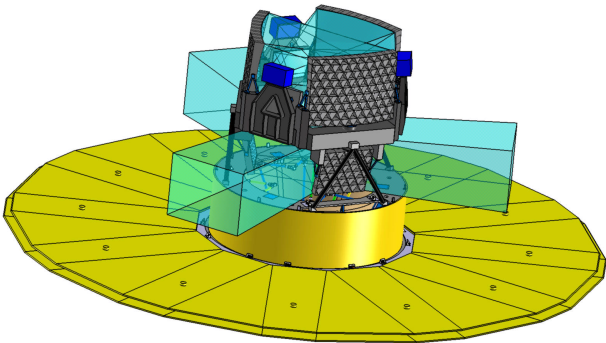


Figure 21: Spacecraft view.

The propulsion sub-system is fully recurrent from *Gaia* and uses chemical bi-propellant standard system

for trajectory control and AOCS coarse manoeuvres, together with fine micro-propulsion system (cold gas) for fine pointing.

Spacecraft electrical architecture

The spacecraft platform architecture is fully based on well-proven and existing technologies, with a maximum reuse from the *Gaia* spacecraft.

- The Data Management System (DMS) is based on the *Gaia* ESA programme. The hardware architecture of the DMS features a state-of-the-art ERC32 central computer (CDMU) in charge of the spacecraft command/control, and an input/output management unit (EIU) for development flexibility: The CDMU interfaces with payload units via a dedicated MIL-STD 1553B bus, and via other spacecraft units via another MIL-STD-1553B bus.

- All spacecraft AOCS is based on the *Gaia* existing baseline, including micro-propulsion.

- All spacecraft chemical propulsion is based on the *Gaia* propulsion system.

- Power management and regulation are performed by the Power Conditioning & Distribution Unit (PCDU) and is based on the *Gaia* program. Electrical power is generated by the recurrent *Gaia* solar arrays (fixed and deployable on the sunshield assembly).

- The RF architecture is also based on the *Gaia* equipments for the transponder and LGA. The *Gaia* active phase array antenna, used to counteract satellite spin, shall be adapted to extend its domain of elevation angle to $\pm 30^\circ$ around a nominal inclination of 40° (instead of $\pm 15^\circ$ around 45° for *Gaia*). The science telemetry output is much lower on PLATO (lower than 0.15 Mbits/s) than on *Gaia*, providing margins on the telemetry link budget and enabling this Active Phase Array antenna modification. A third antenna shall be set-up for cases where the Earth is just behind the spacecraft, and this could be performed with a single fixed MGA ($\approx 20^\circ$ aperture with a TWTA of 65 W RF, reused from Mars Express program. The data produced in one day are downlinked in less than 2.5 hours.

Attitude control

The attitude control is based on the *Gaia* hardware. In spin mode, *Gaia* star detection algorithms are reused to enable the use of the payload star speed measurements in the loop. In staring more, the attitude errors are measured through star barycentre calculation. In spin mode, two detectors per telescope (also used for science) are sufficient for providing the adequate inputs for attitude control purpose. In staring mode, a single detector per telescope is sufficient. The detectors can be selected at field positions with the best optical quality (PSF width $\approx 3.5''$).

In spin mode, it is desirable for simplifying data calibration and ground processing to accurately monitor the telescope line of sight so as to fall on the same macropixel after one satellite revolution. The high signal level enables star speed measurement accuracy better than 5 mas/s (centroiding better than 1/400th of the PSF), with an average measurement rate higher than 30 Hz. When using the three telescope AOCS data, and considering that the system is continuously measuring the same stars the pointing stability can be permanently maintained below $\approx 0.1''$ (1σ).

The spin rate is higher than for *Gaia* and dynamic imbalance will be minimized for maintaining gyroscopic torques below the solar pressure one. This should be eased by the payload natural symmetry.

Spacecraft budgets

The power system generates 1450 W for a 40° sunshield protection angle in worst case of Sun illumination.

Considering *Gaia* figures for the spacecraft mass as pessimistic assumption, the estimated dry mass is 1500 kg dry mass and 2000 kg wet mass at launch, compatible with the Soyuz launch.

The required propellant is estimated to be equivalent to that of *Gaia*, with the same delta-V for the same orbit, and slightly higher chemical propellant need for AOCS manoeuvre, well within the current *Gaia* tanks sizing. Cold-gas propellant is also equivalent to the *Gaia* case (45 kg).

4.2.6 Technological readiness

PLATO SVM is a straightforward re-use of *Gaia* SVM and does not require technology developments. The payload module assembly relies on existing technologies and existing *Gaia* detectors. Therefore no technology developments are required for PLATO for the spinning concept.

4.2.7 Programmatics and costs

The cost estimate of PLATO in the spinning concept is based upon the following assumptions:

- a high-level of recurrence with *Gaia*, both at SVM and payload levels, which results in significant cost reductions, in particular for contingency allocation (16%)
- before consolidated analyses, the effort of development for the scientific ground segment is assumed to be close to that of the staring concept
- the payload external cost (outside ESA part) is lower than in the staring concept, due to a displacement of the "cost barycenter" from FPA chips toward optics.

The reference industrial organization is assumed to be with one prime contractor in charge of delivering the integrated space segment and one prime contractor in charge of delivering the ground segment.

The focal plane assemblies (FPA), the on-board application software and the ground segment data processing algorithms are assumed to be delivered by partner laboratories or subcontractors funded by cooperation and are thus removed from the total estimated cost for ESA.

All costs for spacecraft and payload (equipment, engineering, project office and AIT) were established by EADS Astrium on the basis of ESA equivalent programmes. The total estimated cost includes a 16% contingency margin, also covering design/cost uncertainties at system level at this step of the mission definition.

By default, some budget lines are fitted to the reference Main Cost Elements (MCE) given by ESA for Class M Missions.

The proximity in terms of design, industrial processes and planning between *Gaia* and PLATO encourages to reduce the PLATO contingency margin w.r.t the ESA MCE value.

Activity	ROM (M€)	% of total (ESA part)	Comment
Pre-implementation (studies)	6	2%	ESA MCE
Spacecraft total estimated cost	219		
Spacecraft total industrial cost for ESA	165	54%	
SVM (product, project office, AIT)	100		
Payload (focal plane not included)	65		
Payload on-board software and processing units	9		Cooperation
Focal plane assembly (complete set)	45		Cooperation
Launch services from CSG (SF-2B)	40	13%	ESA MCE
Ground segment total estimated cost	24		
Ground segment total industrial cost for ESA	15	5%	
Calibration and scientific processing chains	9		Cooperation
ESA internal cost	31	10%	ESA MCE
Overall mission cost	320		
Contingency – provision for risks	40	16%	< ESA MCE
Design maturity margin (at mission level)	8		
TOTAL estimated cost with margins	368		
TOTAL estimated cost with margins for ESA	305		

Estimated cost of PLATO in the "spinning" concept

4.3 Advantages of the various concepts

The previous sections show that two different concepts comply with the scientific requirements of PLATO. Both are technologically mature, and can be developed at essentially no risk. In this section, we emphasize the advantages of each one of these concepts. *The staring concept* is based on a design with a large number of identical telescopes. The payload therefore has a very high level of redundancy, and is very robust against failures or defects of one or even several units. The basic observation strategy, which consists of monitoring continuously the same field for several years, with a duty cycle close to 100% and an extreme

stability, allows to reach a very low level of noise. More than 100,000 stars can be observed at a noise level below 2.5×10^{-5} per hr, while about 400,000 stars are monitored at a level $\leq 8 \times 10^{-5}$ per hr. This very low noise on such a high number of targets will allow the detection of exoplanets with sizes significantly smaller than the Earth's, and also the detection of terrestrial planets around stars hotter than the Sun, of spectral type early-F or late-A, thus extending very significantly our statistical knowledge of exoplanet distribution. This concept also enables asteroseismic analysis of all stars monitored by the mission, simultaneously with the transit search.

The spinning concept relies directly on *Gaia* heritage, is highly recurrent with this previous mission, and offers a large degree of redundancy thanks to the use of 96 CCDs. Its main advantage is to allow the detection of exoplanets in all regions of the galaxy, thanks to the scanning strategy, and therefore to study if and how exoplanet distribution depends on the location in the galaxy. At a given magnitude, it will also survey a somewhat larger number of stars than the staring concept, although at lower precision in search mode (*i.e.* in the spinning phase). In particular the spinning concept will allow planet transit search on a large number of very bright and nearby stars.

The existence of two different concepts, which are both *a priori* within the financial limit of a class-M mission, gives a high confidence on the feasibility of the PLATO mission. We believe that the choice of concept should be made early in the assessment phase, after an initial evaluation of both solutions, on both scientific and technological points of view.

4.4 Optional concepts

The two instrumental concepts presented above do not constitute the only solutions to the requirements of PLATO. Optional concepts also exist, and can be more thoroughly examined at the beginning of the assessment phase before a definite trade-off is made between the various concepts. We give here an example of such an alternative concept.

One way of optimizing the search for planets in nearby stars is to cover a large fraction of the galaxy using a wide-FOV camera with very fast optics. There are commercial, off-the-shelf optics available with *e.g.* 50-mm entrance diameter with a focal length of 47.5 mm (f/0.95) and acceptable image quality. The combination of a relative small camera lens with a small, fast readout CCD in frame transfer configuration could result in a very powerful system for planet search pro-

grammes as well as asteroseismology on bright stars. Frame transfer CCDs will allow short integrations and high duty cycle, and the short focal length will ensure a very large FOV. An f/0.95 (50 mm diameter) system equipped with four $1K \times 2K$ ($13 \mu\text{m}$ pixels) CCDs will have a FOV of 32×32 degree². Twelve such cameras will cover the whole galaxy (360×32 degree²). The cameras may be placed on a ring around the spacecraft roll axis, all cameras pointing perpendicularly to the roll axis. In order to increase the collecting area one could install a large number of these rings. Using *e.g.* 25 rings would give a total system of 300 lenses and 1200 CCDs. The total collecting area per FOV will be 0.05 m^2 , which is about 6–7 per cent of the instrument concepts presented earlier. However the total FOV is more than one quarter of the whole sky.

5 Comparison with existing & planned missions

Three space missions have been flown, or are planned for the near future, in the area of exoplanet transits and asteroseismology: the Canadian-led small stellar seismology MOST satellite, launched in 2003, the French-led CoRoT mission for stellar seismology and planet search, launched in 2006, and the US *Kepler* mission, to be launched in 2009. All three missions are expected to bring essential results in these two areas, but suffer limitations in terms of number of stars monitored, minimum planet size, maximum orbital period, precision in frequency measurements for asteroseismology... PLATO, as a next-generation mission after these pioneering experiments, will overcome these limitations, and provide us with a much better, much deeper investigation tool for studying the statistics of exoplanets and their evolution, as well as stellar structure and evolution. Table 7 compares the characteristics of these previous missions with those planned for PLATO.

These previous space missions will leave a strong need for a further mission aiming at establishing a complete and unbiased statistical knowledge of exoplanetary systems. Such is the goal of PLATO.

In particular, in its survey of more than 100,000 stars brighter than $m_V=11-12$, PLATO will bring us the essential capability to characterize completely the stars orbited by the detected planets. This characterization will involve ground-based follow-up observations, but also asteroseismic analysis of these stars, using PLATO data. Such characterization will allow us to measure accurately the radii and masses of the detected planets,

mission	coll. area (m ²)	f.o.v. (deg ²)	monitoring (days)	# stars exo	mag range exo	# stars seismo	mag range seismo
CoRoT	0.057	4	150	60,000	11.5 - 15.5	100	5.5 - 9.5
<i>Kepler</i>	0.7	111	1460	100,000	9 - 14	1400	9 - 11
PLATO 1 staring concept	0.75	400	1825	100,000 400,000	4 - 12 12 - 14	100,000	4 - 12
PLATO 2 spinning concept	0.72	1240	1825 1 min every 20 min	144,000 2,500,000	4 - 11 11 - 14	144,000	4 - 11

Table 7: Comparison of performance of CoRoT, *Kepler*, and the two instrumental concepts envisaged for PLATO.

and will provide a reliable estimate of their ages, as argued in Section 2.2. This is one of the most important advances of PLATO compared to CoRoT and *Kepler*, whose observing strategies are such that they will find planets mainly around faint and distant objects, making it very challenging – if not impossible – to study in detail the characteristics of the exoplanet’s host stars. Also, due to the large distances to these stars, there is no hope for future direct imaging and spectroscopic investigation of the planets discovered by these missions, whereas PLATO should identify potential targets for future interferometric and coronagraphic space- and ground-based instruments.

Moreover, for this sample of 100,000 stars, similar in size as that of *Kepler*, PLATO will reach a noise level at least three times lower than the average level of noise of *Kepler*, and will therefore allow us to detect smaller planets in front of cool dwarf stars, or terrestrial planets in front of hotter and larger stars, thus significantly extending our knowledge of the statistics of exoplanetary systems.

In addition, PLATO is designed to detect terrestrial planets in the habitable zone down to about $m_V = 14$, a performance very similar to that of *Kepler*. Due to the larger size of the surveyed field, PLATO will monitor about 400,000 stars down to this magnitude, extending by approximately a factor of four the sample of detected planetary systems over *Kepler*.

Also, the seismological observations of the proposed concept will give us the possibility to study stellar oscillations down to solar-like level for more than 100,000 stars, of all masses and ages. This is a considerable step forward compared to currently planned missions: it represents 1,000 times the stellar sample monitored by CoRoT, about 100 times that planned for the seismology programme of *Kepler*, and more than five times the sample that was planned for the *Eddington* mission.

This star sample represents a significant fraction of the targets to be observed by *Gaia*/RVS, and for which PLATO will provide an estimate of their age. The

age determination, missing from the *Gaia*/RVS science, will nicely complete the space and velocity-space coordinates provided by *Gaia*, and bring us a full characterization of the surveyed galactic populations.

PLATO, by largely extending the results of CoRoT and *Kepler* in the area of exoplanet search and characterization, and in that of stellar structure and evolution, represents a natural step in our investigation of stellar and planetary system evolution. Filling and extending the important place in the European strategy that was left vacant by the cancellation of *Eddington*, PLATO will complete our knowledge of the statistics of extrasolar systems and stellar evolution. Hence, flying a mission like PLATO after CoRoT, *Kepler* and *Gaia* is a requirement for our understanding of stellar and planetary formation and evolution.

Finally, PLATO observation of bright and nearby stars will make the well-known problem of false alarms for planetary transit search techniques less severe. For instance, background eclipsing binaries, which usually dominate the false alarm problem, will constitute a much smaller difficulty: an eclipsing binary mimicking a planetary transit in front of a star with $m_V = 11$ will need to be 100 times brighter than that mimicking a transit with the same depth for a $m_V = 16$ star, and it can be shown that the probability of false alarm due to such an event will be 100 times lower.

6 International partnership

The overall development strategy assumes that the spacecraft, launch and operations, as well as a major part of the payload, including in particular the telescopes will be provided by ESA. The focal planes, the onboard scientific data treatment, as well as a participation to the ground segment development, will be provided by a consortium involving the US, India, and the European scientific community through national funding by some of ESA member states. There is a

strong interest and expertise in Europe, for instance in France, Spain, and the UK, for the development of focal planes, as well as onboard and ground software for this mission. We give below some details of the anticipated participation of countries outside ESA, as discussed with our colleagues and endorsed by their national space agencies (see attached letters of initial endorsement by NASA and ISRO).

Outside of national European space agencies, PLATO will collaborate mainly with NASA (through the Jet Propulsion Laboratory, JPL) to bring to the mission additional resources as well as personnel experienced in a variety of key areas: instrument hardware, science operations, and scientific contributions.

US Instrument Contribution ($\approx \$30\text{-}35M$, FY10-launch; costs are preliminary and subject to change during the assessment phase):

- During the mission assessment phase, the European and US PLATO teams will identify substantial work packages with clear, well defined interfaces as part of the development of the instrument. The exact work packages and their scope will depend on the selection between the staring and spinning options. The present plan involves the US designing, manufacturing, and testing the integrated Proximity Electronics Modules with a focus on reducing their cost and power dissipation while maintaining critical low noise performance.
- The US would also provide a small number (4) high speed detector assemblies suitable for integration into a standard PLATO camera. Based on hybrid or fully integrated CMOS detectors, these devices would read out (x,y) positions of a few tens of bright stars every ≈ 0.1 second for the rapid, high precision jitter control needed for highest precision photometry.

- The US will study the applicability of backside illuminated CMOS devices with high filling factors for the entire camera package given the potential for significant reductions in power, cost and complexity in the warm electronics compared with CCDs.

- Immediately upon selection, NASA Headquarters, JPL and ESA would develop technology agreements appropriate to exchanging technical information and ultimately providing flight hardware in accord with US ITAR regulations.

US Science Operations ($\approx \$1\text{-}2M/yr$, FY10-End of Mission+1 year):

Personnel at the Michelson Science Center (part of the Infrared Processing and Analysis Center at Caltech/JPL) are experienced in the processing and archiving of large amounts of photometric and astrometric data as well as in developing tools to combine primary mission data with ancillary follow-up infor-

mation. MSC/IPAC personnel have a long history of involvement in ESA science operations, including ISO, Herschel and Planck. In conjunction with the PLATO team, the US would develop a plan for combining PLATO data with pre-launch and post-launch ancillary data. The US data center would also serve as a portal to users of PLATO data in the US.

US Scientific Contributions ($\approx \$1\text{-}2M/yr$, FY10-End of Mission+1 year):

US team members bring a variety of scientific skills and interest to PLATO in the areas of asteroseismology and planetary transits. They would become intimately involved in the preflight planning such as choice of targets fields including some open clusters, as well as spectroscopic characterization of target stars (age, Fe/H, membership); science operations; and ultimate exploitation of the data for scientific purposes, e.g. comparison of asteroseismology ages of PLATO stars with classical determinations, and interpretation of stellar oscillations in terms of fundamental stellar parameters across the full range of stars in the HR diagram.

A significant participation is also expected from the Indian Space Agency, ISRO, and a group of scientific institutes in India. This participation would include the development of the payload central calculator, a participation to the development of the onboard data treatment software, as well as a participation to the scientific exploitation of the data.

In addition to these contributions from the US and India, we are also expecting some scientific contributions from scientists and engineers in Brazil.

7 Communication & outreach

The media interest in PLATO may center on two major aspects of its scientific goals: the detection of exoplanets on one hand, and the interest for the age, size, and content of the Universe on the other. The key result will be centered on the detection of habitable planets and their precise characterization through the detailed analysis of their central stars. Of particular importance will be the seismic analysis of these stars, and their accurate dating.

The general public outreach activities will center on the popularization of the results, by creating and preparing popular material (print articles, broadcast media and web) in which the significance of the mission results and their relevance to astronomy at large will be explained.

Finally, PLATO's outreach activities will target educational institutions. The purpose will be to al-

low students to actually repeat the experiments which will have led to PLATO's discoveries. This will be achieved by making available (on a dedicated web site) pre-processed datasets from among the ones actually observed by PLATO, together with the instructions, description, and software tools necessary to analyze them, allowing students to repeat PLATO's discoveries. It might also be mentioned that PLATO will discover transits of Jupiter-sized planets for relatively bright stars which might be within reach of amateur astronomers or schools equipped with moderately-sized telescopes with CCD cameras. Such follow-up observations of discoveries made by PLATO would clearly be extremely exciting, both to those taking direct part and to the public at large.

References

- [1] Agol, E., Steffen, J., Sari, R., Clarkson, W., 2005, MNRAS 359, 567
- [2] Aerts, C., *et al.* 2003, Science 300, 1926
- [3] Baglin, A., *et al.* 2006, In: *The CoRoT Mission, Pre-Launch Status*, ESA SP-1306, Eds. M. Fridlund, A. Baglin, J. Lochard, L. Conroy p. 11-538
- [4] Baliunas, S.L., Donahue, R.A., Soon, W., Henry, G.W., 1998, ASP CS-154, 153
- [5] Bazot, M., Vauclair, S., 2004, A&A 427, 965.
- [6] Borucki, W.J., *et al.* 2003, ASP CS-294, p. 427
- [7] Bouchy, F., Pepe, F., Queloz, D., 2001, A&A, 374, 733
- [8] Brown, T.M., 2003, ApJ 593, L125
- [9] Carrier, F., Eggenberger, P., Bouchy, F., 2005 A&A 434, 1085
- [10] Charbonneau, D., Brown, T., Noyes, R., Gilliland, R. 2001, ApJ 568, 377
- [11] Christensen-Dalsgaard, J., Däppen, W., Dziembowski, W. A., Guzik, J. A., 2000, in *Variable Stars as Essential Astrophysical Tools*, C. Ibanoglu (ed.), Kluwer, p. 59
- [12] Croll, B., Walker, G.A.H., Kuschnig, R., Matthews, J.M., Rowe, J.F., Walker, A., Rucinski, S.M., Hatzes, A.P., Cochran, W.D., Robb, R.M., Guenther, D., Moffat, A., Sasselov, D., Weiss, W.W., 2006, ApJ 648, 607
- [13] Clementini, G., Gratton, R., 2002, European Review, Vol. 10, Issue 02, p. 237-248
- [14] Deming, D., Harrington, J., Seager, S., Richardson, L., 2006, ApJ 644, 560
- [15] Holman, M.J., *et al.*, 2006, ApJ 652, 1715
- [16] Garrido, R., 2000, In: *δ Scuti and Related Stars*, M. Breger and M.H. Montgomery (eds.), ASP CS-210, p. 67
- [17] Gough, D.O., 1995, In: *GONG 94: Helio- and Astero-Seismology from the Earth and Space*, R.K. Ulrich, E.J. Rhodes Jr., W. Däppen (eds.), ASP CS-76, p. 551
- [18] Grillmair, C., *et al.* 2007, ApJ 658, L115I
- [19] Houdek, G., 2007, In: *SOHO 18/GONG 2006/HELAS I: Beyond the Spherical Sun*, Fletcher, K. (ed.), ESA SP-624, in press
- [20] Israelian, G., Santos, N. C., Mayor, M., Rebolo, R. 2001, Nature, 411,163
- [21] Knutson, H., *et al.* 2007, Nature 447, 183
- [22] Krauss, L.M., Chaboyer, B., 2003, Science 299, 65
- [23] Libbrecht, K.G., 1992, ApJ 387, 712
- [24] Lochard, J., Samadi, R., Goupil, M.J., 2005, A&A 438, 939
- [25] Mermilliod, J.C., Maeder, A., 1986, A&A 158, 45
- [26] Mosser, B., Maillard, J.-P., Bouchy, F., 2003, PASP 115, 990
- [27] Mosser, B., *et al.* 2005, A&A 431, L13
- [28] Namouni, F., 2005, Astron. J. 130, 280
- [29] Pamyathnykh, A.A., Handler, G., Dziembowski, W.A., 2004, MNRAS 350, 1022
- [30] Perryman, M.A.C., Brown, A.G.A., Lebreton, Y. *et al.*, 1998, A&A 331,81
- [31] Richardson, L., Deming, D., Horning, K., Seager, S., Harrington, J. 2007, Nature 445,892
- [32] Robin, A.C., Reylé, C., Derrière, S., Picaud, S., 2003, A&A 409, 523
- [33] Rodonò, M., Lanza, A.F., Catalano, S. 1995, A&A 301, 75
- [34] Roques, F., Moncuquet, M. 2000, Icarus 147, 530
- [35] Roxburgh, I.W., 2004, in *Stellar Structure and Habitable Planet Finding*, 2nd Eddington Workshop, ESA-SP 538, p.23
- [36] Rucinski, S.M., Walker, G.A.H., Matthews, J.M., Kuschnig, R., Shkolnik, E., Marchenko, S., Bohlender, D.A., Guenther, D.B., Moffat, A.F.J., Sasselov, D., Weiss, W.W., 2004, PASP, 116, 826, 1093
- [37] Santos, N.C., 2005, Proc. 13th Cool Stars Workshop, F. Favata *et al.* (eds), in press
- [38] Sartoretti, P., Schneider, J., 1999, A&AS 134, 553
- [39] Schneider, J. 1999a, in F. Paresce (ed.), Proc. of the VLT Opening Symposium Antofagasta, Springer
- [40] Schneider, J. 1999b, C.R. Acad. Sci. Ser. II 327, 621
- [41] Simon, A. Szatmary, K., Szabo, G.M., 2007, A&A, in press
- [42] Udry, S., Bonfils, X., Delfosse, X., Forveille, T., Mayor, M., Perrier, C., Bouchy, F., Lovis, C., Pepe, F., Queloz, D., Bertaux, J.-L., 2007, A&A, in press
- [43] van den Bergh, S., 1995, Science, 270, 1942
- [44] Vidal-Madjar, A., *et al.* 2004, ApJ 604, L69
- [45] Weiss, W.W. 2006, in *The CoRoT Mission Pre-Launch Status*, eds.. M. Fridlund *et al.*, ESA SP-1306, 93-95